SANDIA REPORT
SAND2009-5286
Unlimited Release
Printed August 2009

Molecule-Based Approach for Computing Chemical-Reaction Rates in Upper Atmosphere Hypersonic Flows

Michael A. Gallis, Ryan B. Bond, John R. Torczynski

Prepared by
Sandia National Laboratories
Albuquerque, New Mexico 87185 and Livermore, California 94550

Sandia is a multiprogram laboratory operated by Sandia Corporation,
a Lockheed Martin Company, for the United States Department of Energy's
National Nuclear Security Administration under Contract DE-AC04-94AL85000.

Issued by Sandia National Laboratories, operated for the United States Department of Energy by Sandia Corporation.

Available to DOE and DOE contractors from
U.S. Department of Energy
Office of Scientific and Technical Information
P.O. Box 62
Oak Ridge, TN 37831

Telephone: (865) 576-8401
Facsimile: (865) 576-5728
E-Mail: reports@adonis.osti.gov
Online ordering: http://www.osti.gov/bridge

Available to the public from
U.S. Department of Commerce
National Technical Information Service
5285 Port Royal Rd.
Springfield, VA 22161

Telephone: (800) 553-6847
Facsimile: (703) 605-6900
E-Mail: orders@ntis.fedworld.gov
Online order: http://www.ntis.gov/help/ordermethods.asp?loc=7-4-0#online

SAND2009-5286
Unlimited Release
Printed August 2009

Molecule-Based Approach for Computing Chemical-Reaction Rates in Upper Atmosphere Hypersonic Flows

Michael A. Gallis[1], Ryan B. Bond[2], John R. Torczynski[1]
[1]Microscale Science and Technology Department, [2]Aerosciences Department,
Sandia National Laboratories
P.O. Box 5800
Albuquerque, New Mexico 87185-0346

Abstract

This report summarizes the work completed during FY2009 for the LDRD project 09-1332 "Molecule-Based Approach for Computing Chemical-Reaction Rates in Upper-Atmosphere Hypersonic Flows". The goal of this project was to apply a recently proposed approach for the Direct Simulation Monte Carlo (DSMC) method to calculate chemical-reaction rates for high-temperature atmospheric species. The new DSMC model reproduces measured equilibrium reaction rates without using any macroscopic reaction-rate information. Since it uses only molecular properties, the new model is inherently able to predict reaction rates for arbitrary non-equilibrium conditions. DSMC non-equilibrium reaction rates are compared to Park's phenomenological non-equilibrium reaction-rate model, the predominant model for hypersonic-flow-field calculations. For near-equilibrium conditions, Park's model is in good agreement with the DSMC-calculated reaction rates. For far-from-equilibrium conditions, corresponding to a typical shock layer, the difference between the two models can exceed 10 orders of magnitude. The DSMC predictions are also found to be in very good agreement with measured and calculated non-equilibrium reaction rates. Extensions of the model to reactions typically found in combustion flows and ionizing reactions are also found to be in very good agreement with available measurements, offering strong evidence that this is a viable and reliable technique to predict chemical reaction rates.

TABLE OF CONTENTS

LIST OF FIGURES

LIST OF TABLES

NOMENCLATURE

b	scattering parameter	(pure)
c_r	relative speed	$(\mathrm{m/s})$
C_1, C_2	cross section parameters	(pure)
E_t	translational energy	(J)
E_i	internal energy	(J)
$E_c = E_t + E_i$	collision energy	(J)
i	vibrational energy state	(pure)
$K_{eq,r}$	equilibrium reaction constant	(pure)
k	reaction rate	$(\mathrm{m^3 molecule^{-1} s^{-1}})$
k_B	Boltzmann constant	$(\mathrm{J/K})$
m	mass	(kg)
q	temperature exponent in Park's model	(pure)
r	distance	(m)
T	temperature	(K)
z_v	vibrational partition function	(pure)
Z_i	vibrational relaxation number	(pure)
Z	non-equilibrium reaction rate parameter	(pure)

Greek

α	VSS angular scattering parameter	(pure)
Γ	gamma function	(pure)
ε_i	specific internal energy of mode i	$(\mathrm{Jkg^{-1}})$
ε	symmetry parameter	(pure)
ζ	degrees of freedom	(pure)
Θ_d	characteristic dissociation temperature	(K)
Θ_v	characteristic vibrational temperature	(K)
Λ	reaction rate constant	(pure)
μ	viscosity	$(\mathrm{Nsm^{-2}})$
ν	IPL distance exponent	(pure)
σ	cross section	$(\mathrm{m^2})$
ϕ	fraction of collisions exchanging internal energy	(pure)
χ	scattering angle	(deg)
ω	viscosity temperature exponent	(pure)

Acronyms

ADM	Adiabatic Dissociation Model
CCI	Contracted Configuration Interaction
CE	Chapman-Enskog
CVD	Chemical Vapor Deposition
DSMC	Direct Simulation Monte Carlo
GLB	General Larsen-Borgnakke
IPL	Inverse Power Law
ME	Maximum Entropy
M-F	Macheret and Fridman

M-T	Marrone and Treanor
PVD	Physical Vapor Deposition
QCT	Quasi-Classical Trajectory
TCE	Total Collision Energy
VHS	Variable Hard Sphere
VSS	Variable Soft Sphere

Subscripts

a	activation
b	backward
c	collision
d	dissociation
eq	equilibrium
i	internal energy mode
max	maximum
mol	molecule
R	reaction
r	reduced for mass, relative for speed
ref	reference
rot	rotational
t	total
tr	translational
vib	vibrational
1	first order
∞	infinite order

1. INTRODUCTION

There is an ever growing number of technologically important areas in gas dynamics such as hypersonic reentry, materials processing and micro-systems for which the gas is not in thermal equilibrium and cannot be characterized by a single temperature. In cases where non-equilibrium gas flows include chemical processes, these occur in an environment very different from the thermal equilibrium environments in which traditional chemical processes take place. For processes in thermal non-equilibrium, established chemistry models, based on the equilibrium Arrhenius rates $k(T)$, cannot be used since the concept of describing the flow using a single temperature T is no longer valid.

The challenges of modeling chemical reactions in a non-equilibrium environment can be exemplified by the case of hypersonic reentry into the earth's atmosphere (Bird 1994, Park 1990, Dressler 2001) and other planetary atmospheres (Gallis and Harvey 1998). Modeling chemical and ionization reactions at the extreme conditions of hypersonic flow in the upper atmosphere has been a very important problem since the first Apollo-era space flights. However, even today this problem evades a satisfactory solution. The root cause for the inadequate state of modeling is the difficulty in obtaining reliable, internal-energy-state-specific, experimentally measured cross sections for atmospheric species reactions that can be used to validate theoretical models. Efforts by Park (1990, 1993), Gupta et al. (1990), and Bortner (1969) to compile a set of chemical reaction rates that could be used for hypersonic applications were hampered by this lack of measurements.

It is indicative of the scarcity and inadequacy of the measurements, even under conditions of thermodynamic equilibrium, that for the so-called, first Zeldovich reaction, $N_2 + O \rightarrow NO + N$, one of the most important reactions in hypersonic flow fields and one of the reactions considered best known, measurements exist only in the regime between 2,384 K-3,850 K. These conditions are vastly different from the non-equilibrium conditions at temperatures in excess of 15,000 K typically met in hypersonic applications. Given the paucity of measurements, current Arrhenius-type chemical reaction rates (Park 1990, Bortner 1969, Gupta et al. 1990) used for hypersonic flow fields are based at best on extrapolations of measured low-temperature equilibrium rates and at worst on estimations from radiation data. For some of the reactions of interest, no experimental data exist, and the reaction rates are mere estimates based on reactions between other species, after having their rates adjusted to reflect the differences in the equilibrium collision frequency.

The state of knowledge for the rates of atmospheric-species reactions under conditions of thermodynamic non-equilibrium is even less advanced. The behavior of atmospheric chemical reactions under conditions of thermal non-equilibrium has not been systematically investigated, and using equilibrium chemical-reaction data in gas dynamics codes to simulate thermal and chemical non-equilibrium in hypersonic flow fields can lead to unknown and potentially large errors in their predictions. Park (1990), in an attempt to include non-equilibrium effects into the calculation of chemical reaction rates, used information from experimental observations and flight data and conjectured that the available reaction-rate data could be better fitted by an Arrhenius-type two-temperature model. According to Park's model, replacing the gas

temperature in the Arrhenius rate by the geometric average of the translational and the vibrational temperature of the gas could sufficiently account for non-equilibrium effects.

Park's model has since been the principal method for dealing with non-equilibrium flows within the framework of the Navier-Stokes equations although the suggested mechanisms employ a considerable degree of empiricism. Further research with Park's model has focused on better estimating the dependence of the reaction rate on the energy content of the molecular energy modes and more specifically on the temperatures characterizing the vibrational and the translation modes. Concerns have been voiced (Gupta et al. 1990, and references therein), mainly based on quantum mechanical calculations, that the selection of temperatures and the weighting of the temperature by the vibrational temperature may not provide a good representation of the actual conditions. For example, it is believed that excitation of the vibrational mode promotes slow endothermic reactions but influences fast endothermic reactions to a lesser extent (Chernyi et al. 2004).

Physico-chemical approaches to quantify the effect of thermodynamic non-equilibrium on chemical reaction rates led to a number of semi-theoretical or semi-empirical models (Chernyi et al. 2004). These models, lack the generality of the Park model since they are applicable to a particular type of chemical reactions, and they calculate the non-equilibrium reaction rates $k(T_{tr}, T_{vib}, T_{rot}, T_{el})$ as a deviation from the equilibrium reaction rate $k(T)$ using the form $k(T_{tr}, T_{vib}, T_{rot}, T_{el}) = k(T)Z(T_{tr}, T_{vib}, T_{rot}, T_{el})$, where the subscripts tr, vib, rot, el stand for the translational, vibrational, rotational, and electronic energy modes, respectively. These models are useful tools to theoretically describe and evaluate the importance of various competing mechanisms in promoting a reaction. The disadvantage of these models is that the reaction rates, at best estimated from low-temperature equilibrium data, are being used, making the non-equilibrium reaction-rate predictions highly questionable and of unknown accuracy.

The most widely used method for simulating fluid flows uses the continuum fluid mechanics Navier-Stokes equations, which for continuum near-thermodynamic-equilibrium gas dynamics can be derived from the Boltzmann equation based on the perturbation analysis of Chapman and Enskog (Chapman and Cowling 1970). The Navier-Stokes equations, which are physically well founded for continuum near-equilibrium flows, are the most computationally efficient method for gas dynamics. The problem with simulating chemically reacting flows with the Navier-Stokes equations is that all the available computational models implicitly or explicitly depend on the thermal-equilibrium Arrhenius rates. This limits the applicability of the Navier-Stokes equations to the regime where the particular compilation of Arrhenius rates can be trusted.

Unlike Navier-Stokes codes, which require chemical-reaction-rate models as inputs, molecule-based techniques such as the Direct Simulation Monte Carlo (DSMC) method (Bird 1994), which deals with individual molecules and their collisions, can simulate gas flows at a more fundamental level that is closer to reality. The DSMC method is capable of simulating non-equilibrium gas behavior based on kinetic theory that calculates molecular collisions using stochastic rather than deterministic procedures as in Molecular Dynamics. This improves the computational efficiency of DSMC greatly compared to other Monte Carlo and "particle" methods. As a result, Bird's Direct Simulation Monte Carlo (DSMC) method is used almost universally in rarefied gas dynamics and whenever mean-free-path phenomena are of interest.

Two molecules in an intermolecular collision are unaware of the macroscopic temperature of the gas, and the outcome of their collision is controlled only by their orientation, their energy content and its distribution among the available modes of the colliding pair. Therefore, for a chemical-reaction-rate model to be physically realistic and reliable for non-equilibrium flows, it is of paramount importance that it depends only on molecular-level processes and does not rely on equilibrium or macroscopic information. Within the framework of DSMC, an approach for determining chemical-reaction rates from first principles and fundamental microscopic molecular data has recently been developed (Bird 2009) that obviates the need for any macroscopic rate information. These molecular processes can be used not only to model highly non-equilibrium chemically reactive flows within the context of DSMC but also to develop chemical-reaction-rate models for near-continuum flows that can be used by Navier-Stokes continuum fluid dynamics codes.

Energy exchanges during molecular collisions and chemical reactions are closely connected. Both Newton's equation of motion for a classical system and Schrödinger's equation for a quantum system are unchanged by time reversal. Due to this symmetry under time reversal, the probability of a forward chemical reaction from a particular energy state taking place is equal to the probability of this energy state appearing in the products of the reverse reaction. This concept, termed the principle of *microscopic reversibility* or *reciprocity theorem* (Reif 1965), is key to the development of chemical reaction models. The statistical relationship between the rate constants for forward and reverse reactions at equilibrium resulting from microscopic reversibility is known as the principle of *detailed balance*. Thus, before examining the chemical reaction mechanisms, the mechanisms of inter-molecular energy exchange and the corresponding DSMC models will be reviewed.

2. MODELING GAS FLOWS WITH DSMC

DSMC uses a molecule-based, stochastic algorithm to approximate the continuous molecular velocity distribution function with a discrete number of computational molecules, or "simulators" (Bird 1994). It has been theoretically shown (Wagner 1992) that the DSMC algorithm provides an exact solution to the Boltzmann equation in the limit of infinite simulators and vanishing discretization errors (time step and cell size). The simplicity of the DSMC algorithm is one of its most attractive features. DSMC uses computational molecules that move, reflect from walls, and collide with each other to simulate the noncontinuum behavior of a dilute gas under the assumption of molecular chaos. Each computational molecule typically represents a large number of real molecules.

The basic assumption of DSMC is that the molecular motion and collision phases can be decoupled, which is appropriate when the time step is much smaller than the mean collision time. Thus, the molecular motion and the collisions that take place simultaneously are broken into two cyclically repeated parts. This separation reflects the processes described by the left and right sides of the Boltzmann equation (convective and collision parts), respectively. It is noted that the Boltzmann equation, when originally proposed by Boltzmann, was based on physical arguments similar to those used to describe DSMC.

Macroscopic quantities are determined by sampling moments of the velocity distribution within each mesh cell over one or more time steps. Sampling in the standard DSMC algorithm takes place after collisions are performed. However, sampling can be done either before collisions or both before and after collisions. If the flow is statistically steady, long-time averages can be used to reduce statistical uncertainty (the ergodic hypothesis).

During a time step, each molecule moves ballistically at its velocity. The time step is selected so that it is smaller than the mean time between collisions. Molecules that cross a solid boundary during the move phase are reflected back into the computational domain. These reflections can be specular, diffuse at the wall temperature, diffuse without energy change, or a linear combination of these (in a probabilistic sense).

Between moves, pairs of molecules within each cell are randomly selected to collide at the appropriate rate. The stochastic collisions of computational molecules reproduce the statistics of collisions of real molecules. In the established DSMC algorithm (Bird 1994), collision candidates are selected from anywhere within a computational cell. However, refinements of the collision algorithm have been implemented where neighboring molecules are preferentially selected for collision (Bird et al. 2009).

2.1 Modeling Collisions

Collision dynamics are treated by molecular collision models that provide a compromise between physical realism and computational efficiency. The Hard-Sphere (HS) model (Bird 1994) represents molecules with velocity-independent diameters, which experience isotropic scattering. The Variable Hard Sphere (VHS) model (Bird 1994) is an extension that allows the diameters of colliding molecules to depend on their relative speed but retains isotropic scattering.

The Variable Soft Sphere (VSS) model (Bird 1994) is a further extension that allows anisotropic scattering. The HS, VHS, and VSS potentials are spherically symmetric (although the scattering is anisotropic except for HS and VHS molecules), whereas real molecules have asymmetric potentials. Under the assumption of molecular chaos (Bird 1994), the angular orientations of pre-collision molecules are uncorrelated. Since DSMC collisions represent the statistics of large numbers of real collisions, the asymmetry is averaged out, making the spherical representation a reasonable one. The most important feature of any model is that the variation of the collision cross section with relative speed, which is related to the viscosity of the gas, is adequately captured. Although more complicated molecular models than VSS and VHS can be devised, these simple models are preferred since they adequately reproduce the viscosity of the real gas over a wide temperature range. Other parameters, such as the scattering angle, have a relatively smaller effect on observable gas properties.

In the DSMC simulations, the VSS interaction is used to approximate the Inverse-Power-Law (IPL) interaction. VSS represents the hard-sphere interaction exactly and provides a good approximation to IPL interactions, which are point centers of a repulsive force that varies with the intermolecular separation r as $1/r^{\nu}$. Both the IPL and VSS molecular interactions yield thermal conductivities and viscosities with a T^{ω} temperature dependence where $\omega = 1/2 + [2/(\nu - 1)]$. The VSS interaction uses a molecular diameter d that depends on the relative molecular speed c_r according to $d \propto c_r^{-2/(\nu-1)}$. For a gas that has a viscosity coefficient proportional to T^{ω} and with a reference viscosity of μ_{ref} at temperature T_{ref}, Chapman-Enskog (CE) theory allows for the reference molecular collision "diameter" d_{ref} to be related to the viscosity of the gas by the following expression:

$$d_{\mathrm{ref}} = \left(\frac{5(\alpha+1)(\alpha+2)(mk_B T_{\mathrm{ref}}/\pi)^{1/2}}{4\alpha(5-2\omega)(7-2\omega)\mu_{\mathrm{ref}}(\mu_1/\mu_\infty)} \right)^{1/2}, \tag{1}$$

where μ_∞/μ_1 is the CE infinite-to-first-approximation ratio of the gas viscosity. Here, α is the angular-scattering parameter, which relates the scattering angle χ to the impact parameter b according to $b \propto \cos^{\alpha}[\chi/2]$. Since $\alpha = 1$ produces isotropic (hard-sphere) scattering, the VHS interaction uses this value for all ω values (i.e., for all IPL interactions). The VSS interaction uses different values of α to represent different IPL interactions. The α value that achieves the best match between the VSS and IPL interactions is determined by equating the VSS and IPL Schmidt numbers (the Schmidt number is $\mu/\rho D$, where μ is the viscosity, $\rho = mn$ is the mass density, and D is the self-diffusion coefficient):

$$\alpha = (2A_2[\nu])/(2A_1[\nu] - A_2[\nu]), \tag{2}$$

where $A_1[\nu]$ and $A_2[\nu]$ are functions in Chapman and Cowling (1970). From these equations, the values $\alpha = 1$ and $\alpha = 2.13986$ are obtained for hard-sphere and Maxwell molecules, respectively. It is emphasized that the values $\omega = 1/2$ and $\alpha = 1$ exactly reproduce the hard-sphere interaction (VSS and VHS are identical in this situation) but that the VSS values $\omega = 1$ and $\alpha = 2.13986$ (and the VHS values $\omega = 1$ and $\alpha = 1$) only approximate the IPL Maxwell interaction.

These molecular models have been very successfully used in DSMC since, despite their simplicity, they predict monatomic molecular transport properties very accurately both under conditions of equilibrium (Gallis et al. 2004) and non-equilibrium (Gallis et al. 2006). Gallis et al. (2004) demonstrate that DSMC using the VSS molecular model can reproduce the infinite order solution of the CE theory for transport properties of monatomic species. It is also important to note that these models are computationally efficient, especially when compared to the more realistic but also computationally more demanding counterparts such as the Lennard-Jones or Morse potentials (Hirschfelder, Curtiss, and Bird 1954).

2.2 Modeling Internal Energy

Molecular simulation techniques such as DSMC are particularly useful when considering non-continuum phenomena in gases, primarily because these processes originate at the molecular level. DSMC inherently treats all molecular energy modes separately and is amenable to considering different relaxation rates and quantum effects. In fact, considering such effects with molecular techniques is much simpler than with macroscopic techniques since the best understanding of these processes is provided by theory (quantum mechanics, molecular relaxation theory) at the molecular level.

A computationally efficient way of treating polyatomic species is to add polyatomic-molecule features to monatomic-molecule models. Thus, the VHS and VSS models are extended to polyatomic molecules by adding internal degrees of freedom to the three translational degrees of freedom along with a method for exchanging translational and internal energy. Similar to the translational mode, an internal energy mode is characterized by ζ, its number of degrees of freedom, and the exchange method is characterized by τ, the relaxation time, or its microscopic equivalent, ϕ, the fraction of collisions exchanging internal energy with translational energy. The collision number $Z_i = 1/\phi$, the average number of collisions between exchanging internal and translational energy, is usually prescribed (Bird 1994, 2009).

For a complete description of molecular collisions with internal energy modes, molecular simulation methods require cross sections for all allowable transitions between energy states (translational and internal). However, due to the large number of such transitions, this approach is cumbersome to implement in a molecular dynamics code, even assuming that all cross sections are known. In fact, the collision dynamics between polyatomic molecules are poorly understood, with very little information available.

Instead of a detailed cross-section treatment of molecular interactions, DSMC uses phenomenological models and conservation principles to describe collisions. These models approximate the cross sections in a way that leads to equipartition between the available energy modes and that yields a Maxwellian distribution function at equilibrium. The approximate cross sections need not be particularly accurate representations of the real ones. In fact, in the absence of experimental or theoretical information for most of these cross sections, a detailed evaluation of these DSMC procedures is not possible. The model procedures are required to account for all the degrees of freedom, produce the correct relaxation rate, and satisfy the principle of reciprocity (reversibility) between transitions at the microscopic level or detailed balance at the macroscopic level.

During an inelastic collision of polyatomic molecules, energy is exchanged between the internal and the translational modes. Since the cross sections for these collisions are in general not available, the phenomenological General Larsen-Borgnakke (GLB) model (Bird 1994) is almost universally used in DSMC simulations. According to this model, the internal energies after an inelastic collision are reassigned by sampling from the total energy equilibrium distributions, given below:

$$f\left(\frac{E_{tr}}{E_c}\right)=\frac{\Gamma\left[5/2-\omega+\zeta\right]}{\Gamma\left[5/2-\omega\right]\Gamma\left[\zeta\right]}\left(\frac{E_{tr}}{E_c}\right)^{3/2-\omega}\left(1-\frac{E_{tr}}{E_c}\right)^{\zeta-1}, \tag{3}$$

$$f\left(\frac{E_i}{E_c}\right)=\frac{\Gamma\left[5/2-\omega+\zeta\right]}{\Gamma\left[5/2-\omega\right]\Gamma\left[\zeta\right]}\left(1-\frac{E_i}{E_c}\right)^{3/2-\omega}\left(\frac{E_i}{E_c}\right)^{\zeta-1}, \tag{4}$$

where E_{tr} is the total translational energy, E_i is the total internal energy, $E_c = E_{tr} + E_i$ is the total energy of the colliding pair of molecules (conserved in the collision), and Γ is the gamma function. The molecular model enters the equilibrium distributions through ω, thus differentiating the equilibrium distribution of the molecules that constitute the gas from the distribution of the colliding molecules (Bird 1994).

Unlike the rotational energy mode, a typical vibrational mode has energy states that are widely spaced compared to typical translational energies, so the vibrational mode is not fully excited. Thus, a continuous description of the energy states is not appropriate, and a quantized description must be used instead. The actual spacing of discrete energy states or a model that describes their spacing is needed. Two models, each of which includes contributions from potential and kinetic energy (i.e., $\zeta_{\text{vib}} = 2$), for the discrete energy states of the vibrational mode of a diatomic molecule are the harmonic oscillator,

$$\varepsilon_{vib,i} = ik_B\Theta_v,\ i = 0,1,2,\ldots,\ \Theta_v = 3374.2\ \text{K}, \tag{5}$$

and the anharmonic oscillator which according to the equation of Herzberg (Bird 1994),

$$\varepsilon_{vib,i} = k_B\left\{T_A\left[\left(i+1/2\right)-c_2\left(i+1/2\right)^2+c_3\left(i+1/2\right)^3\right]-T_B\right\},\ i = 0,1,2,\ldots,$$
$$T_A = 3395\ \text{K},\ T_B = 1692.3\ \text{K},\ c_2 = 0.006126,\ c_3 = 0.00000318, \tag{6}$$

where Θ_v is the characteristic vibrational temperature and all values are for molecular nitrogen.

For low temperatures, namely nitrogen at $T \le 1000$ K, these two models yield almost identical results because only the first few vibrational energy states are populated to any observable degree. Herein, the harmonic oscillator is used.

The Boltzmann distribution for the vibrational energy ε_v of energy state i is given by

$$f(E_{vib}) \propto \delta\left[E_{vib} - ik_B\Theta_v\right]\exp\left[-E_{vib}/k_BT\right]. \quad (7)$$

The GLB model therefore is applied as for the continuous modes with the exception that the random selection of the potential energy content of vibrational mode is made using Equation (5) i.e., an integer energy state i from 0 to the maximum allowable energy state $E_c/\left(k_B\Theta_v\right)$ is randomly selected. The rest of the model is applied in the same way regardless of how the energy of the state was calculated.

It should be noted here that the energy selection in a particular collision does not take place using the local (cell-wise) equilibrium distribution function. The equilibrium distribution function used in the GLB model is that at a "temperature" based on the total available collision energy, not the cell-average temperature. Effectively, selecting from this equilibrium distribution is a recognition of the fact that collisions lead the gas to equilibration, although multiple collisions are needed to reach it. In this way, an effective non-equilibrium behavior is produced.

It is clear that more assumptions are made for polyatomic molecules than for monatomic molecules. Some of them, such as the assumption of a spherical potential, are not immediately obvious. The lack of exact theoretical results (resulting from the inability to formulate and solve the Boltzmann equation for realistic polyatomic-molecule potentials) precludes a verification study of the type performed previously for monatomic molecules (Gallis et al. 2004). Instead, DSMC simulations are compared to experimental results. Comparisons between actual and DSMC values of transport properties over the temperature range typically encountered indicates that very good agreement between DSMC models and experimental data can be achieved (Bird 1994).

3. MODELING CHEMICAL REACTIONS IN DSMC

Molecular-level modeling is ideally suited to the study of chemically reacting gas flows. As such, DSMC procedures entirely based on microscopic properties of the colliding molecules and completely unaware of the macroscopic conditions of the surrounding gas can provide flow-field predictions under arbitrary conditions of non-equilibrium. As outlined in Section 2, DSMC procedures for intermolecular collisions employ a cross section that is a function of the relative translational energy of the colliding molecules. It is through Chapman-Enskog theory that this cross section can be related to the temperature-dependent viscosity of the real gas, a physical quantity that can be readily measured. Thus, it is not necessary to introduce a macroscopic temperature to model the translational mode during molecular collisions.

To model chemical reactions within the context the DSMC method, complete tabulations of the cross sections as a function of the impact parameters and energy states of the molecules are needed. Such information could come from quantum mechanical calculations, supported by experiment. However, very little such information is available, and that limited information applies to only a small number of reactions. The complexity of the situation almost guarantees that there will be no significant increase in the amount of such information available in the foreseeable future.

In the absence of such detailed data, DSMC simulations have to resort to phenomenological models, conceptually similar to those used to model intermolecular interactions, that capture the most essential features of the microscopic mechanisms while maintaining the computational efficiency of DSMC. In a similar fashion to the molecular models used in DSMC, chemistry models aim to reproduce the main properties of the chemical-reaction processes but in a computationally efficient manner. A necessary, but not sufficient, condition for any chemistry model to be valid is its ability to reproduce the equilibrium reaction rates. More advanced features include linking the energy-exchange process to that of chemical reactions and satisfying the principles of macroscopic reversibility at a microscopic level and detailed balance at the macroscopic level.

3.1 DSMC Chemistry Models

There are many possible ways that DSMC chemistry models can be categorized. Herein, the DSMC models will be partitioned into two main categories: models that use macroscopic equilibrium rate information to calibrate adjustable parameters, and models that use only microscopic and collision-specific information without resorting to adjustable parameters. The former comprise a very large number of models of varying sophistication and complexity. The latter consist of the work by Bird (1994, 2009). DSMC chemistry models have been reviewed and comparatively evaluated on many occasions (Dressler 2001, Wadsworth and Wysong 1997).

3.1.1 Models Based on Arrhenius Rates

A necessary condition for any model is to be able to reproduce measured Arrhenius reaction rates. Thus, the first model for chemical reactions in DSMC was proposed by Bird (1979) was based on satisfying this requirement. This model, termed the Total Collision Energy (TCE)

model, provides a microscopic reaction model that can reproduce the conventional macroscopic Arrhenius rate equation in the continuum limit. According to this model a generic form for the reaction cross section is assumed:

$$\sigma_R = \sigma_T C_1 (E_c - E_a)^{C_2} \left(1 - E_a / E_c\right)^{\bar{\zeta}+3/2-\omega_{AB}}, \tag{8}$$

where σ_T is the total cross section for the particular molecular model used, E_a is the energy threshold of the reaction, E_c is the total collision energy, $\bar{\zeta}$ is the average number of internal degrees of freedom, and C_1 and C_2 are constants. Integrating this cross section over the available collision energy E_c, Bird obtains a chemical-reaction-rate coefficient in the Arrhenius form:

$$k(T) = \Lambda T^{\eta} \exp(-E_a / k_B T). \tag{9}$$

By comparing the temperature exponent and the Λ factor, two equations are obtained that can be used to define the two adjustable parameters, C_1 and C_2. The model, based on considerations of mathematical tractability, is evidently phenomenological in nature. This model has been used extensively in DSMC simulations and produces results that are in good agreement with measurements (Bird 1994).

Marriott and Harvey (1990) propose a model termed the Maximum Entropy (ME) method based on the work of Levine and Bernstein (1987). According to the ME method, the reaction probability depends on the distribution of the internal energy (vibrational, rotational, electronic) among the reactants. This approach makes use of the concept of microscopic reversibility in the energy disposal after a reaction by linking the energy dependence of the reaction probability of the forward reaction to the energy disposal of the reverse reaction. For example, the vibrational mode is considered to be particularly efficient in promoting dissociation reactions (Levine and Bernstein 1987). Thus, it would be physically preferable if the reaction probability was associated with the energy stored in the vibrational mode, instead of the total collision energy. By doing so and to ensure that the system is microscopically reversible, it is required that, when energy is distributed after a recombination reaction (the reverse of a dissociation reaction), the products preferentially populate the vibrational mode at the level that the dissociation reaction would require to proceed, so that at equilibrium a steady state can be achieved. Gallis and Harvey (1996) demonstrate that the ME and GLB methods can be combined to produce the desired effect of using energy-distribution probability density functions to predict chemical reaction probabilities.

However, the ME model shares the same disadvantage as the TCE model and its variants, namely that it requires suitable experimental data to estimate its adjustable parameters for each reaction. In a similar fashion to the TCE model, a form of the reaction and energy-exchange cross section is assumed, and known experimental data are reproduced using the adjustable parameters within the model. The application of the model is limited by the lack of appropriate experimental data necessary to exploit the proposed model to its full potential.

The suggestion that particular energy modes may play a more important role in determining the probability of a chemical reaction taking place was central to many other models, some of them variants of the TCE model, proposed for use in DSMC (Dressler 2001, Wadsworth and Wysong 1997). A common feature of all these models is the assumption of a particular form of the reaction cross section, a function of the total as well as particular energy modes, and the requirement that these cross sections reproduce a known Arrhenius-type reaction rate. In some cases these models are compared to measured or calculated cross sections. Comparisons of the predictions of the TCE model and its variants for non-equilibrium calculated cross sections for exchange reactions (Dressler 2001, Chapter 3) indicates that the calculated cross sections are of the correct order, which provides some basis for optimism that the non-equilibrium predictions of the model can be considered reliable within the expected error of the method. However, caution must be exercised since detailed cross-section and rate comparisons by Wysong et al. (2002) indicate that extracting adjustable parameters from measured or extrapolated equilibrium reaction rates may lead to unphysical reaction cross sections. Regardless of the ability of these methods to produce physically realistic cross sections, the fact that all these models rely on a limited database of experimental data mostly in the equilibrium regime casts doubts about their ability to cope with highly-non-equilibrium conditions successfully.

3.1.2 Models Based on Microscopic Data

A set of molecular-level chemistry model-processes for use in DSMC has been proposed by Bird (1994, 2009). These processes are based solely on fundamental properties of the colliding molecules, including the available collision energy, molecular dissociation energies, and quantized vibrational energy levels. These event-driven processes link chemical-reaction cross sections to the energy-exchange process and the probability of transition between vibrational energy states. Application of the GLB procedures for collisions between molecules that could lead to endothermic dissociation reactions is conceptually straightforward, whereas for exchange reactions it is more speculative. These procedures and the principle of microscopic reversibility are then used to calculate simple event-driven models for recombination and for the reverse (exothermic) reactions that do not require any macroscopic data with a procedure that seeks to balance the flux into and out of each state.

3.1.3 Dissociation and Recombination Reactions

The introduction of quantum vibrational states in DSMC procedures (Bird 1994) proved to be a significant improvement since it allowed a more realistic representation of the energy in the lower widely-spaced vibrational energy levels. The next step was to link the vibrational excitation to the dissociation procedures. Bird (1994) suggests that dissociation reactions are part of the process of energy exchange between the colliding molecules. In the light of this, the exchange of vibrational energy is incomplete and inconsistent without linking it to molecular dissociation. This concept is captured in an energy threshold model proposed by Bird (1994). According to this model, if during the energy-exchange process of a diatomic molecule the energy content of the vibrational mode exceeded the energy threshold of the dissociation or exchange reaction, the reaction would occur.

Lord (1998) in his critique of Bird's (1994) model points out that there is a "continuum", i.e., an infinite number of states above the dissociation limit. Therefore, Lord argues, if a dissociation reaction is energetically possible, it occurs. Thus, assuming a particular collision between two molecule-simulators, where at least one of them is a molecule, the serial application of the GLB energy exchange model would make energy

$$E_c = E_{trans,pair} + E_{vib,mol} \tag{10}$$

available to the vibrational mode of the molecule in question. In Equation (10), $E_{trans,pair}$ is the translational energy of the pair and $E_{vib,mol}$ is the vibrational energy of the molecule in question. Assuming a harmonic oscillator model for the vibrational mode, the maximum vibrational level that could be obtained $i_{\max}$ is $i_{\max} = \text{int}[E_c/(k\Theta_v)]$. If this level is higher than the dissociation level $i_d = \Theta_d/\Theta_v$, where Θ_d is the characteristic dissociation temperature, i.e., if, $i_{\max} > i_d$, a dissociation reaction occurs.

Assuming a gas in thermodynamics equilibrium at temperature T and a molecule from this gas at a particular vibrational level i, the probability of the translational energy exceeding the difference between the level i and the dissociation level i_d is given by (Bird 1994)

$$P = \frac{\Gamma\left[(5/2-\omega),(\Theta_d - i\Theta_v)/T\right]}{\Gamma(5/2-\omega)} \equiv Q\left[5/2-\omega,(\Theta_d - i\Theta_v)/T\right], \tag{11}$$

where Γ is the incomplete gamma function. Summing these probabilities for all vibrational levels up to the dissociation level i_d, multiplying by the equilibrium collision frequency, and dividing by the number densities of the species, the dissociation rate coefficient is obtained:

$$k(T) = \frac{2\sigma_{ref}}{\varepsilon\sqrt{\pi}}\left(\frac{T}{T_{ref}}\right)^{1-\omega}\left(\frac{2k_B T_{ref}}{m_r}\right)^{1/2}\sum_{i=0}^{i_d}\left\{Q\left[\left(\frac{5}{2}-\omega\right),\left(\frac{\Theta_d - i\Theta_v}{T}\right)\right]\right\}\frac{\exp\left(-i\Theta_v/T\right)}{z_{vib}(T)}, \tag{12}$$

where $z_{vib} = \left\{1-\exp(-\Theta_v/T\right\}^{-1}$ is the vibrational partition function in the harmonic oscillator model, σ, ω, and m_r are the collision cross section, viscosity temperature exponent, and reduced mass of the pair, respectively, and ε is a symmetry parameter that is set to 1 for like molecules and to 2 for unlike molecules.

The model does not explicitly account for the effect of rotational energy participating in the dissociation process. It is known that high rotational energies can stimulate dissociation both by reducing the dissociation energy threshold due to the centrifugal effect and by affecting the dynamics of collisions between rapidly rotating molecules. However, because rotational and translational energies quickly equilibrate, the rotational energy may effectively participate in the process through the translational energy according to Equation (10).

For the fraction of collisions that can be regarded as three-body collisions, the condition for recombination is as follows. Recombination occurs in a collision between the appropriate atoms if the potentially recombined molecule after a trial GLB redistribution of the relative

translational energy of the atom-atom pair is found to be at the ground vibrational state. The addition of the dissociation energy to this molecule would then bring it to the state appropriate for dissociation. A three-body collision is considered to occur if a third molecule-simulator is found within the collision volume of a colliding pair. There is no unambiguous definition of the collision volume. For the purposes of this study and treating the radius of a molecule as its sphere of influence, the collision volume of a colliding molecule is assumed to be that of a sphere having as radius the effective radius of the colliding atoms. The ratio of the collision volume to the cell volume gives the probability that a molecule-simulator is found inside this volume, i.e., within the sphere of influence of the colliding atoms. A third molecule-simulator is not actually selected from the population of the cell to take part in this three-body collision. Instead, the recombination probability is based on the properties of the two initial atoms. Thus, the third colliding partner does not have any effect on the available energy of the collision.

Bird (2009) also proposed a different variant for calculating the probability of recombination reactions based on the principle of microscopic reversibility. According to this principle, the fraction of all dissociating molecules at each vibrational level is sampled separately for each pair of collision partners. For the fraction of atom-atom collisions that could result in the formation of a molecule, a provisional GLB redistribution of the relative translational energy and reaction energy is performed, resulting in a particular vibrational level for the potentially formed molecule. The probability of recombination of the pair equals the probability of dissociation from that vibrational level. Evidently, this model cannot be applied in a single-cell setting where a particular reaction is modeled in isolation of all the other reactions that take place concurrently in the gas.

3.1.4 Endothermic and Exothermic Exchange Reactions

Similarly, endothermic exchange reactions take place when the vibrational level of the colliding molecule after a trial GLB redistribution of energy E_c, as given by Equation (10), is one level above the level corresponding to the activation energy E_a:

$$i = i_a = \text{int}\left[E_a / k_B \Theta_v\right] + 1, \tag{13}$$

where i_a is the first vibrational level above the energy threshold of the reaction.

For example, for an endothermic exchange reaction such as $N_2 + O \rightarrow NO + N$ with activation energy E_a, a reaction takes place if, in an N_2 and O collision, the vibrational level of N_2 after a redistribution of energy is above the reaction activation energy level. The activation energy of the exchange reaction is much smaller than that of the dissociation reaction. The macroscopic rate at which this process occurs can be readily derived:

$$k(T) = \frac{2\sigma_{ref}}{\varepsilon\sqrt{\pi}} \left(\frac{T}{T_{ref}}\right)^{1-\omega} \left(\frac{2k_B T_{ref}}{m_r}\right)^{1/2} \exp\left(-\frac{i_a \Theta_v}{T}\right) \Big/ z_{vib}(T). \tag{14}$$

Physically realistic molecule-level processes such as these can be implemented in standard DSMC codes. This approach makes no use of any macroscopic reaction-rate data and bases the calculation of the dissociation, recombination, and exchange reaction cross sections on kinetic theory and known microscopic data. The fact that the model is introduced in an inherently non-equilibrium method means that arbitrarily chosen non-equilibrium conditions mimicking those encountered by hypersonic vehicles can be simulated and the reactions rates calculated for those conditions.

The law of mass action could be used to determine the cross section of the reverse exothermic reaction, but an event-driven approach based on the principle of microscopic reversibility has overwhelming advantages. Bird (2009) suggests that an exothermic exchange reaction takes place when the newly formed molecule after a GLB trial redistribution of the total collision energy including the reaction energy E_a is formed at the vibrational state corresponding to the activation energy as in Equation (13).

The phenomenological mechanism for the reverse, exothermic reactions could also be formed in a manner similar to the recombination reactions. Thus, an energetically equivalent mechanism would require that the condition for the reverse, exothermic, exchange reaction to take place is that the potentially newly formed molecule after a trial GLB redistribution of the available relative translational and vibrational energy is found to be in the ground vibrational state. Then the energy released during the reaction can be added to the vibrational mode to bring it to the state where the forward reaction is possible. Although the two schemes appear to be similar in terms of the final distribution of energy in the products, they result in different probability density functions for the reaction probability. This is due to the non-linearity of the GLB distributions as a function of energy. However, both mechanisms result in reaction rates of the same order of magnitude. This is indicative of the ability of these phenomenological models to capture the correct order of magnitude of reaction rates although the precise mechanism may not be mimicking exactly the details of the interaction.

4. APPLICATION TO PARTICULAR REACTIONS

In this chapter, the validity of the event-driven approach is investigated by selecting a reduced-chemistry system representative of hypersonic reacting flows for which suggested reaction rates exist. The reliability and accuracy of these rates can be argued. In fact, very few of these reactions have error estimations, and all of them are highly questionable at temperatures above 10,000 K. Nonetheless, this data set represents state-of-the-art knowledge for the rates of these reactions.

In Section 4.1, DSMC reaction rates calculated under conditions of thermodynamic equilibrium are compared against available measurements to confirm that the proposed approach can produce reliable results. Comparisons to actual cross sections would be ideally needed to evaluate the new model. However, rate information is more commonly used and therefore more easily accessible for all reactions of interest. Subsequently, in Section 4.2, the new method is used to produce non-equilibrium reaction-rate information model appropriate for comparison to non-equilibrium chemical reaction rates, semi-empirically or semi-theoretically derived, and to experimentally measured rates. For the second set of comparisons, the vibrational energy is distributed according to the Boltzmann (equilibrium) distribution but at a different temperature than the translational-rotational mode. Finally, Sections 4.3 and 4.4 present comparisons between the DSMC-predicted reaction rates and measured rates for combustion and ionization reactions. The aim of these comparisons is to assess the generality of the DSMC procedures and confirm that whatever agreement is observed in Sections 4.1 and 4.2 is not limited to atmospheric species and hypersonic-entry conditions.

The DSMC chemistry model procedures are implemented in a zero-dimensional DSMC code. Since the collision phase in DSMC is a procedure that involves only molecules within a cell, unlike the move phase, only a single cell need be considered. When two or more simulators are picked for collision, the probability of a chemical reaction occurring is calculated. Through a comparison with a random number, the decision is made as to whether or not a chemical reaction should occur. If it does, the number of reactions is advanced by one, but, unlike ordinary practice, the identities of the molecule simulators are not changed. All the results presented herein were obtained using 10^6 molecule-simulators, with their properties sampled from the equilibrium distribution at the appropriate temperature. To enhance the statistical sample, and only for the equilibrium temperature cases, molecules after a collision are allowed to redistribute their energy between the available modes. For the non-equilibrium case, energy exchange was allowed only between the three degrees of freedom of the translational mode, keeping the total translational energy of the molecule constant while redistributing it among its three components.

It should be noted that, whatever energy redistribution between the colliding molecules is employed, since the zero-dimensional code does not involve interactions with solid boundaries, the system is adiabatic, and the total energy of the cell remains constant and equal to the initial energy of the cell throughout the calculation. This may have a visible effect for high-temperature simulations of low-energy threshold reactions, where a relatively small statistical variation of the total energy may lead to a small but measurable deviation of the equilibrium collision and reaction rate from the equilibrium one.

The development of the DSMC procedures within the context of a zero-dimensional code facilitates its straightforward implementation in any DSMC code, regardless of its serial or parallel nature.

DSMC models for chemical reactions initially dealt with chemical reactions in atmospheric air, mainly reactions between nitrogen and oxygen. Nitrogen, which for most traditional chemical reaction processes is considered to be an inert gas, becomes chemically active under conditions of hypersonic reentry (temperatures around 10,000 K). The chemical reactions in atmospheric air are dominated by dissociation of the diatomic nitrogen and oxygen molecules and exchange reactions between molecules and atoms. Subsequently, DSMC models for more complicated species and chemical reactions were developed to address chemical vapor deposition (CVD) and physical vapor deposition (PVD) applications.

4.1 Equilibrium Reaction Rates for Atmospheric Reactions

The ability to reproduce known equilibrium reaction rates is a necessary condition for any chemistry model. The compilation of reaction rates by Park (1990) is currently considered the most reliable set of reaction rates available. Most of the experimental data, on which the reaction-rate set is based, were obtained for low temperatures (2,000-7,000 K). Park (1990), through careful study and comparison with numerical simulations, suggests that the experimentally obtained reaction rates can be extrapolated up to 30,000 K, if necessary. Due to the variety of measurement techniques and methodologies used in obtaining these rates, the accuracy of the measurements cannot be easily determined. According to Park, most of these rates should be considered reliable within a factor of 3-10. In some cases, significantly different fittings of the Arrhenius-rate functional form to the same data have been presented.

4.1.1 Dissociation Reactions

The main dissociation reactions in hypersonic applications are the dissociation of O_2 and N_2 and to a lesser extent, due to its small concentration, NO. Having a lower dissociation threshold, O_2 is the first species to react, followed by N_2. Due to the low dissociation threshold of O_2, its dissociation reaction has been studied more thoroughly than any other reaction. Adequate measurements also exist for the dissociation of nitrogen. The dissociation of nitric oxide is not as well known. Although nitric oxide is a molecule that can be detected through radiation, its dissociation rate is not well known due to competing reactions that take place. Figures 1-3 present the dissociation reactions of O_2, N_2, and NO. Figures 4-6 present the dissociation reaction rates of the same species due to collisions with atomic oxygen and atomic nitrogen.

The red lines and circles represent the results obtained using the new model with its analytical expression, Equation (12), and its DSMC implementation, respectively. The blue lines represent the reaction rates suggested by Park using his two-temperature model. The green lines represent the experimental measurements Park used to derive his set of reaction rates using a multi-temperature model.

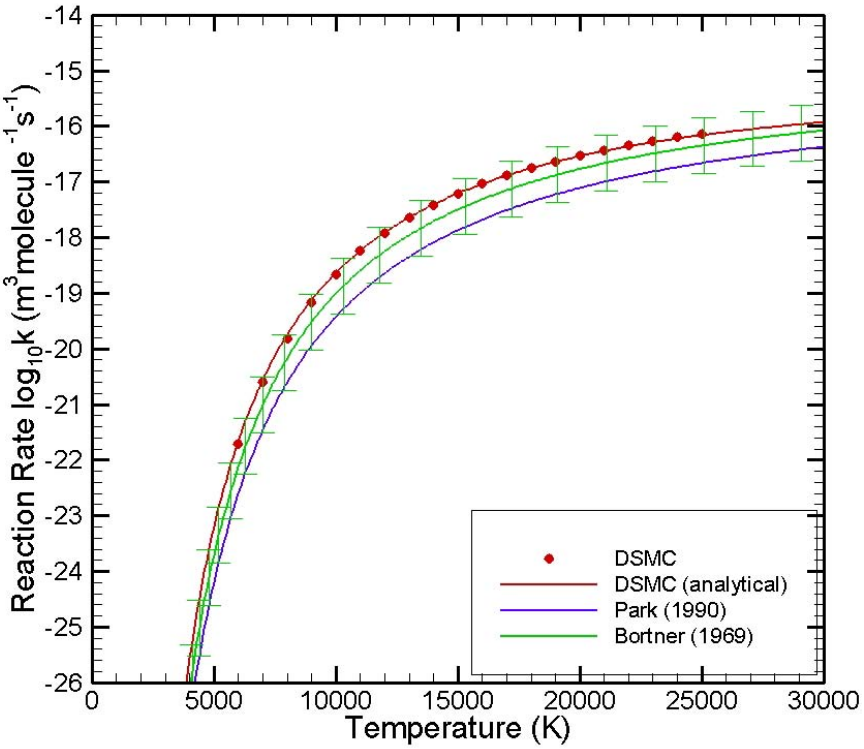

Figure 1. Nitrogen dissociation: $N_2 + N_2 \rightarrow N + N + N_2$.

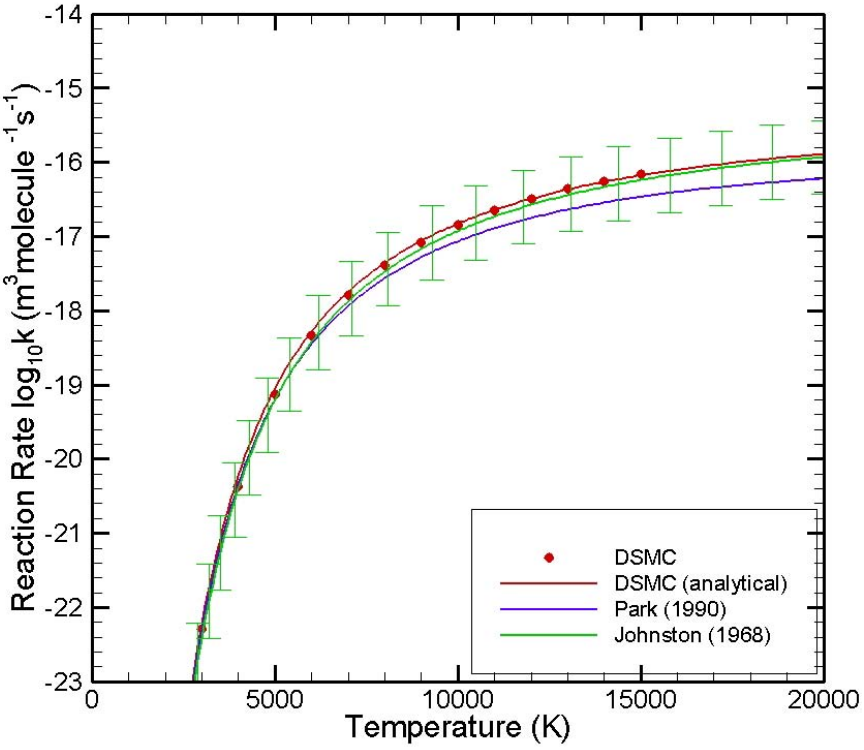

Figure 2. Oxygen dissociation: $O_2 + O_2 \rightarrow O + O + O_2$.

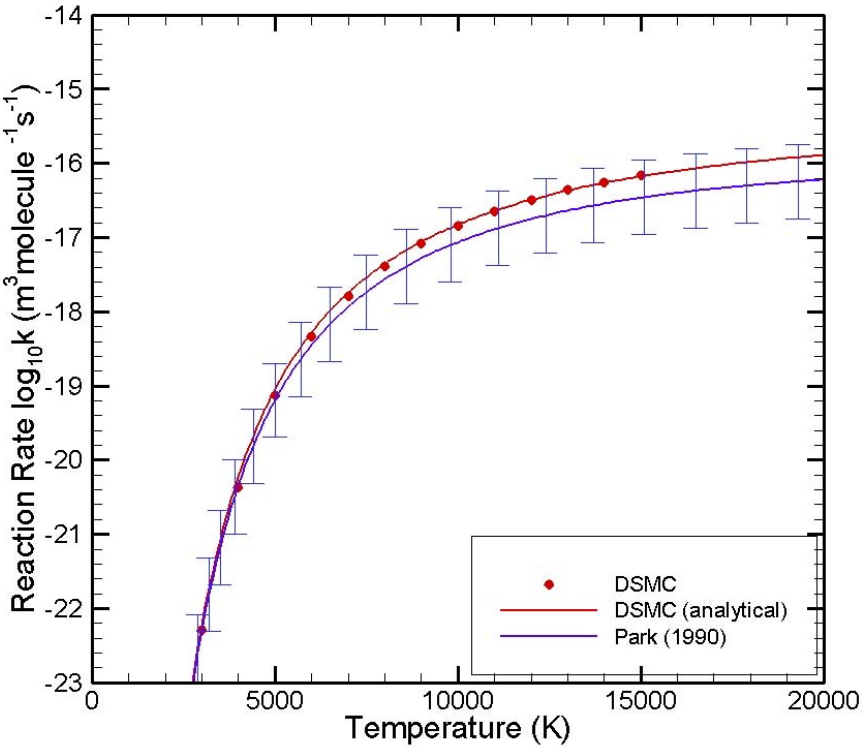

Figure 3. Nitric oxide dissociation: $NO + NO \rightarrow N + O + NO$**.**

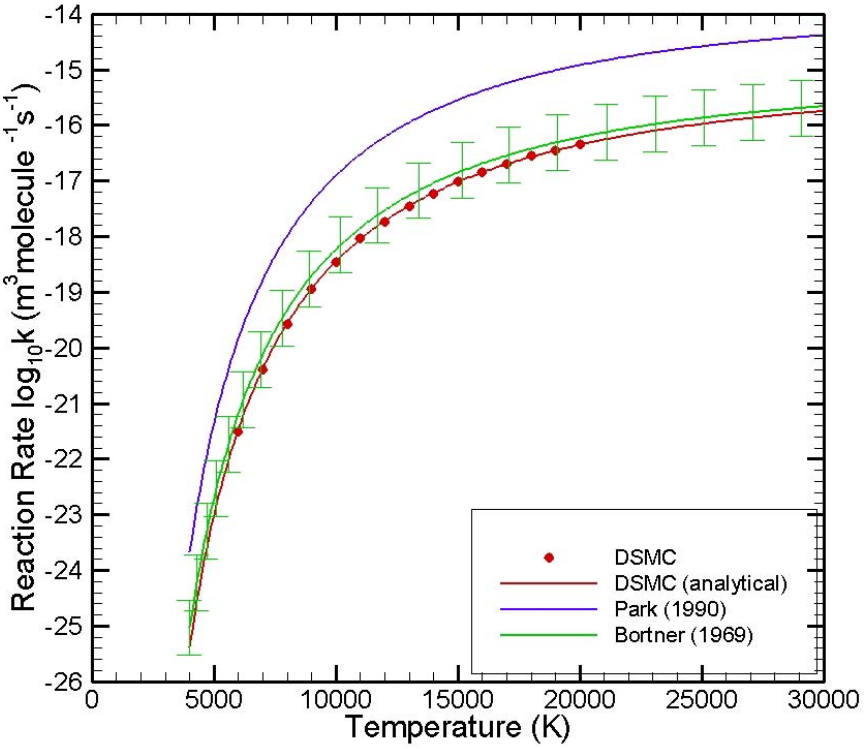

Figure 4. Nitrogen dissociation by atomic nitrogen: $N_2 + N \rightarrow N + N + N$**.**

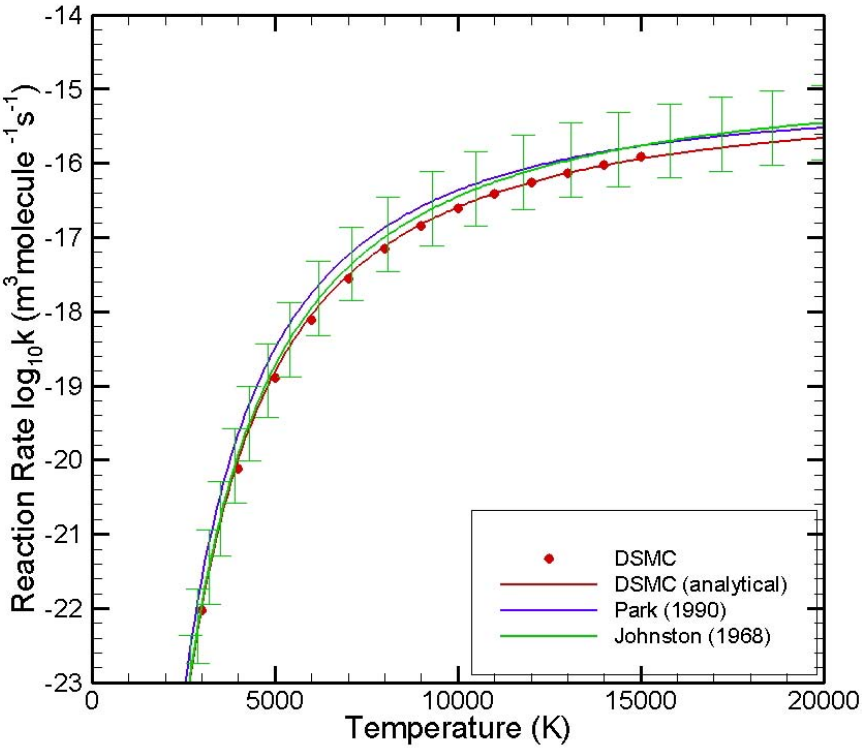

Figure 5. Oxygen dissociation by atomic oxygen: $O_2 + O \rightarrow O + O + O$ **.**

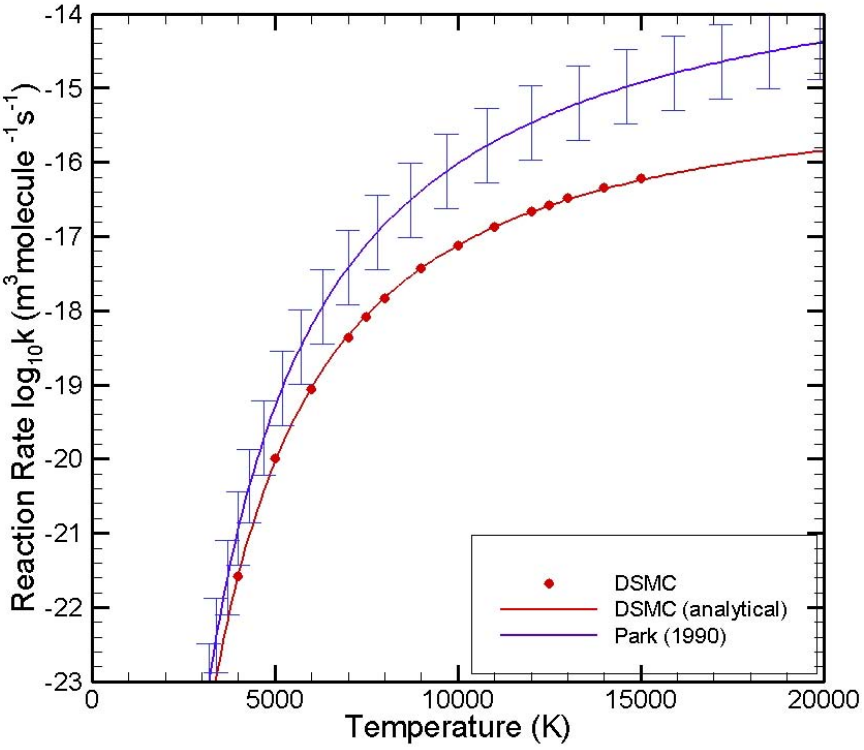

Figure 6. Nitric-oxide dissociation by atomic nitrogen: $NO + N \rightarrow 2N + O$ **.**

It is indicative of the uncertainty related to these rates that the single-temperature interpretations of the original data are different from Park's two-temperature interpretation, which is almost invariably used for hypersonic applications. In Figures 1-6, the rates are extrapolated to either 30,000 K or 20,000 K. Park suggests that, in a real non-equilibrium flow field, the vibrational temperature is always lower than the translational temperature. Thus, even in cases where the translational temperature reaches 50,000 K, the vibrational temperature hardly reaches 10,000 K (at that temperature, O_2 is completely dissociated), bringing the geometric average temperature to about 20,000 K. Extrapolating these rates to 30,000 K, which is significantly above the range where measurements exist, must be considered questionable.

The accuracy associated with these measured rates is not always reported and in some cases not even known. The problem becomes even more severe in the temperature range ($T \geq 10,000\,\mathrm{K}$) where these rates are extrapolated. Park reports that some of the measured reaction rates, for the same reaction, differ by more than one order of magnitude. Based on this observation and for the purpose of facilitating meaningful comparisons with calculated rates, measured and extrapolated reaction rates are herein assumed to be accurate to one order of magnitude. Thus, an uncertainty of one order of magnitude has been assigned to measured and extrapolated rates in Figures 1-6. This uncertainty is designated by error bars.

Based on this presumed accuracy of all measurements, DSMC results (points or solid lines) are generally in good agreement with Park's rates. In fact, the DSMC results may actually be in better agreement with the original data than with Park's interpretation of them. The differences between Park's interpretation of the data and the original data themselves are in almost all cases within the range of uncertainty associated with the measured data. It is not clear therefore, whether the observed better agreement of the DSMC results with the original data can be considered systematic or fortuitous.

Based on the results of Figures 1-6, no unambiguous conclusion can be drawn about the effect of the absence of the rotational energy from the formulation of the model. While atom-molecule dissociation reactions appear to be under-predicting equilibrium reaction rates, exactly the opposite is observed for molecule-molecule reactions.

4.1.2 Recombination Reactions

Recombination reactions are the reverse of dissociation reactions and are usually ignored in typical rarefied hypersonic applications due to their low probability of occurrence. Figures 7 and 8 present the recombination reaction rates of atomic oxygen and atomic nitrogen as functions of temperature at equilibrium conditions. For this type of reaction, no analytical representation of the DSMC model is available. The DSMC rates are compared with the reaction rates given by Gupta et al. (1990). Gupta et al. (1990) provide a better fit to the equilibrium reaction constant K_{eq}, calculated using the partition-function approach of Park (1990). The reaction rates Gupta et al. (1990) provide are based on their fit of the equilibrium reaction constant and the data of Bortner (1969). As in the previous section, in Figures 7 and 8 an uncertainty of one order of magnitude has been assigned to the measured rates to indicate the relative error of the proposed procedures.

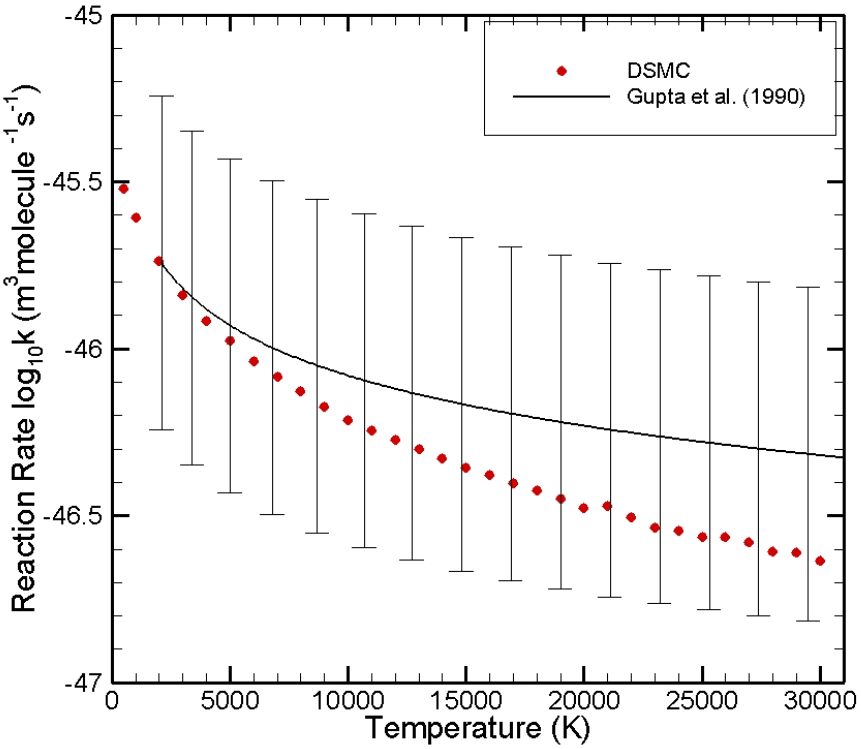

Figure 7. Atomic oxygen recombination: $O + O + O \rightarrow O_2 + O$ **.**

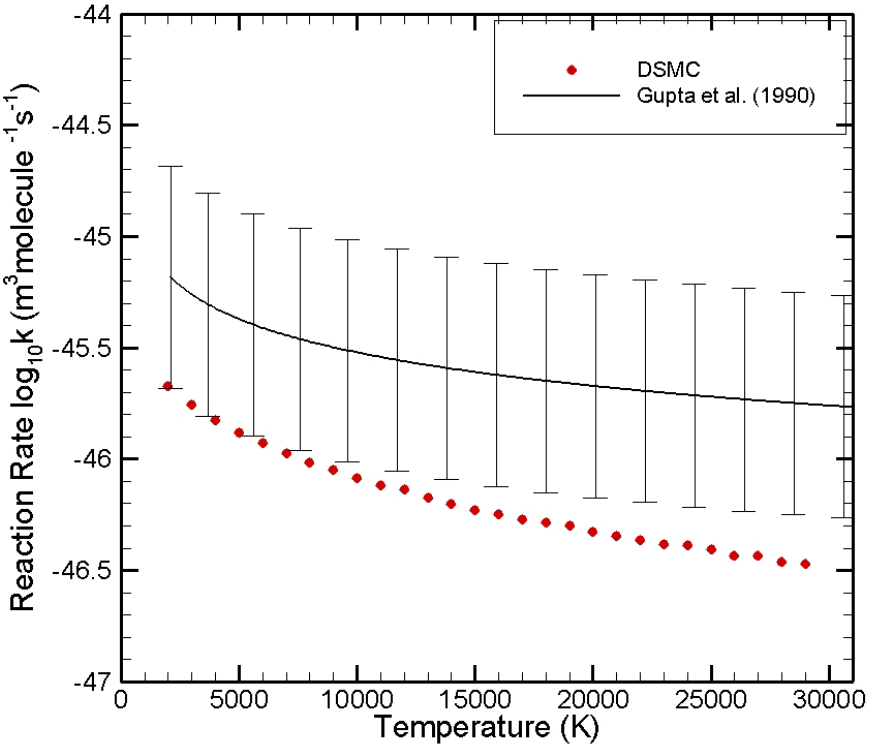

Figure 8. Atomic nitrogen recombination: $N + N + N \rightarrow N_2 + N$ **.**

The oxygen recombination rate is in good agreement with the rate proposed by Gupta et al. (1990). A larger difference, but still less than one order of magnitude, which is the presumed accuracy of the measured rates, is observed for the case of nitrogen recombination.

The model for recombination reactions has the disadvantage of using the ambiguous collision volume (Section 3.1.3) to calculate the three-body collision rate. Bird (2009) assumed the radius of the collision volume to be about 2-3 times the radius of the molecule. As stated in Section 3.1.3., herein, the radius of a DSMC molecule-simulator is assumed to be its sphere of influence, which is thus employed as the radius of the collision volume. Assuming a larger volume would raise the collision probability and therefore the reaction rates, bringing the DSMC nitrogen recombination reaction rate into better agreement with the rates calculated using the equilibrium reaction constant and the measured reverse reaction rates for all temperatures. Similarly, in the vicinity of 15,000 K, using the larger collision volume would bring the oxygen recombination rate into better agreement with the rates calculated using the equilibrium reaction constant and the measured reverse reaction rates.

4.1.3 Endothermic Exchange Reactions

Figures 9 and 10 present the reaction rates of the endothermic exchange reactions

$$N_2 + O \rightarrow NO + N\,, \tag{15}$$

$$NO + O \rightarrow O_2 + N\,, \tag{16}$$

or the Zeldovich reactions, as they are also known (Park 1990). These reactions are critical for hypersonic applications since, because of their low energy threshold, they are mainly responsible for the formation and depletion of nitric oxide, which is a major radiating species in hypersonic flow fields. For both reactions, DSMC predictions are found to be in very good agreement with the measured rates.

The differences between the Park (1990) rates and the measured rates become significant for these reactions, especially at high temperatures. These reaction rates have been measured only at relatively low temperatures, below 4,000 K. Park, based on a variety of data and numerical simulations, proposes a reaction rate with an arbitrary value for the temperature exponent of -1 and suggests that this should be reliable up to 30,000 K. Park also suggests that, for hypersonic flows where the temperature reaches a value of 30,000 K, the vibrational temperature should be limited to around 7,000 K, resulting in an average temperature of 15,000 K. The rate for the reaction in Equation (15) is also compared to the rate measured by Monat et al. (1978). The measured reaction rate has an uncertainty of about 35% in the temperature range 2,384-3,850 K and thus is considered (Park 1990) to be one of the best known reaction rates. Other measurements for this reaction are all within a factor of 3. Since the error of these rates in the extrapolated region of the temperature domain is not known and in harmony with Park's suggestions, all measured and extrapolated rates are assumed to be accurate to within one order of magnitude. This is reflected by the one-order-of-magnitude-wide error bars assigned to the measured rates in Figures 9-14.

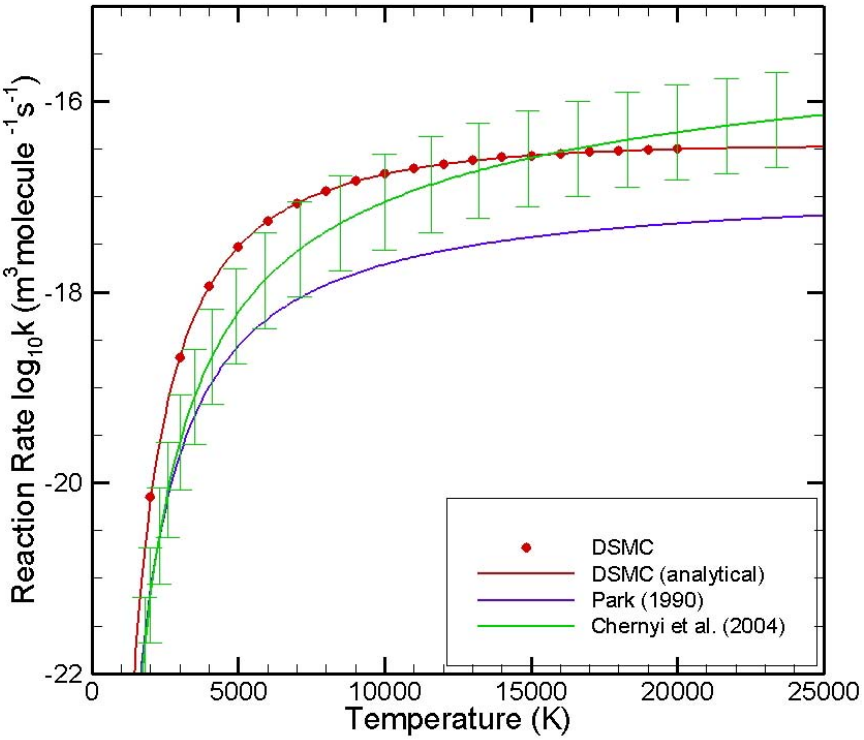

Figure 9. Nitric-oxide/oxygen endothermic exchange reaction: $NO + O \rightarrow O_2 + N$ **.**

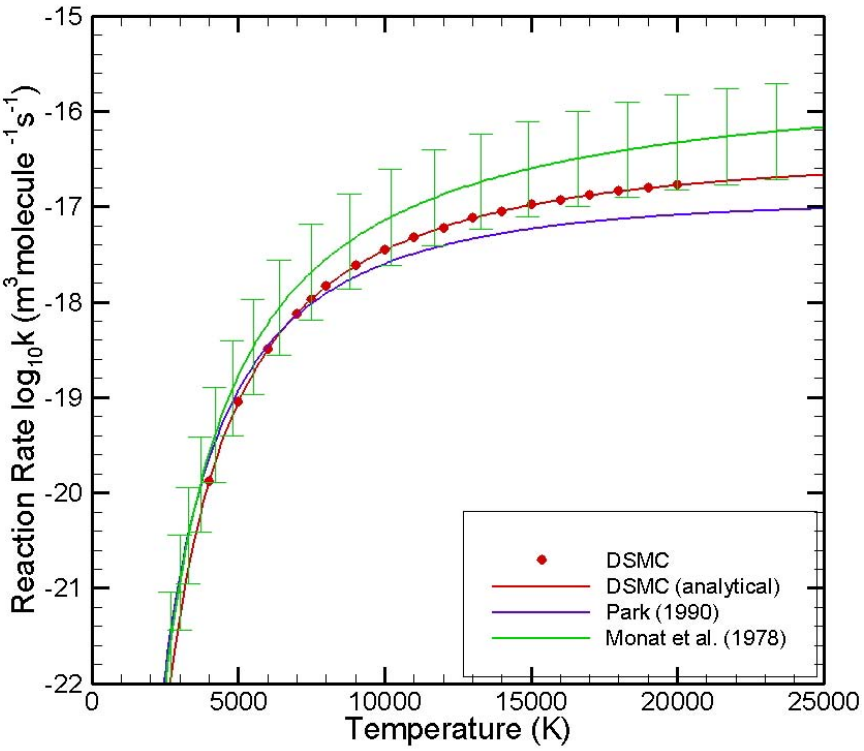

Figure 10. Nitrogen/atomic-oxygen endothermic exchange reaction: $N_2 + O \rightarrow NO + N$ **.**

The DSMC rate at 3,800 K was found to differ by 51% from the measured value. Although this difference is marginally outside the bounds of measurement error, it is well within the one-order-of-magnitude error projected for these reactions.

4.1.4 Exothermic Exchange Reactions

Exothermic exchange reactions are the reverse of the reactions studied in the previous section, namely Equations (15) and (16). No direct measurements for these reverse reactions exist, the reaction rates being estimated from the equilibrium gas constant and the forward reaction rate. Both Park's and Gupta's equilibrium reaction constants are compared the DSMC results in Figures 11 and 12. In both figures, the red symbols present the DSMC reaction rates.

Figure 11 presents the reaction rates for $O_2 + N \rightarrow NO + O$. Gupta et al. (1990) suggest that the reaction rate is constant: $k = 2.4909 \times 10^{-17}$ $m^3 molecule^{-1} s^{-1}$ $(\log_{10}(k) = -16.60)$. The results in Figure 11 are obtained using Park's equilibrium reaction rate constant and Park's and Monat's suggested forward reaction rates.

Figure 12 presents the reaction rates for $NO + N \rightarrow N_2 + O$. Here, the rates suggested by Park and Gupta et al. are compared to the DSMC rates. The different trend of the Gupta et al. rate in Figure 12 is due to a small energy threshold that appears in the reaction rate. No explanation is given for the appearance of this term in the reverse reaction rate. However, in both cases, the DSMC predictions are in reasonable agreement (within one order of magnitude difference) with the theoretical/experimental predictions.

A prominent difference between the DSMC and measured rates is that the DSMC rate increases more gradually with temperature at low temperatures, especially for the reaction $NO + N \rightarrow N_2 + O$ presented in Figure 12. Using the equilibrium reaction constant, a more rapid increase is observed. In fact, according to the equilibrium reaction constants, the rate peaks around 1,000 K and decreases from that point on. The DSMC model produces a more gradual increase up to 5,000-10,000 K, after which the rate appears to plateau. Assuming that these reverse reaction rates are accurate within one order of magnitude, the DSMC model appears to be in fairly good quantitative agreement with Gupta's rates. For the reverse reactions, Gupta's rates should be considered more accurate than Park's rates since they represent a more rigorous implementation of Park's model (Gupta et al. 1990).

If the alternative mechanism for exothermic exchange reactions is used, the DSMC model produces the results shown in Figures 13 and 14. Although both mechanisms produce similar order-of-magnitude results, the second model yields declining rates as a function of temperature in contrast to Bird's model. Although these results (Figures 13-14) appear to be in better qualitative agreement with the measured rates than the original ones (Figure 11-12), the differences between these rates and the measured ones appear to be within their presumed accuracy, so no unambiguous conclusion on the superiority of any of these models can be made based on this comparison.

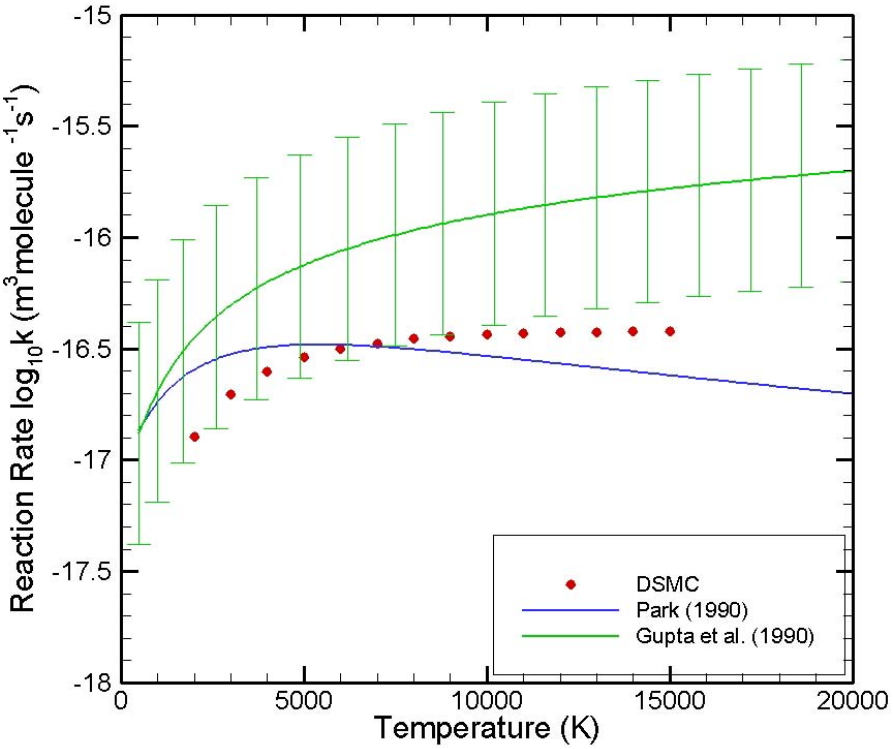

Figure 11. Oxygen/atomic-nitrogen exothermic exchange reaction: $O_2 + N \rightarrow NO + O$ **.**

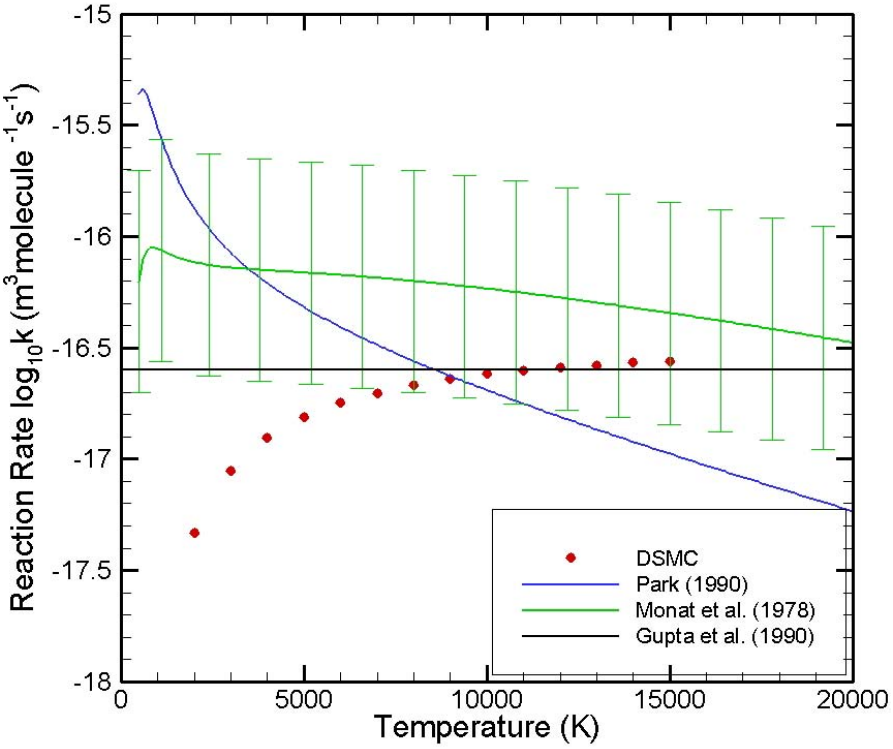

Figure 12. Nitric-oxide/atomic-nitrogen exothermic exchange reaction: $NO + N \rightarrow N_2 + O$ **.**

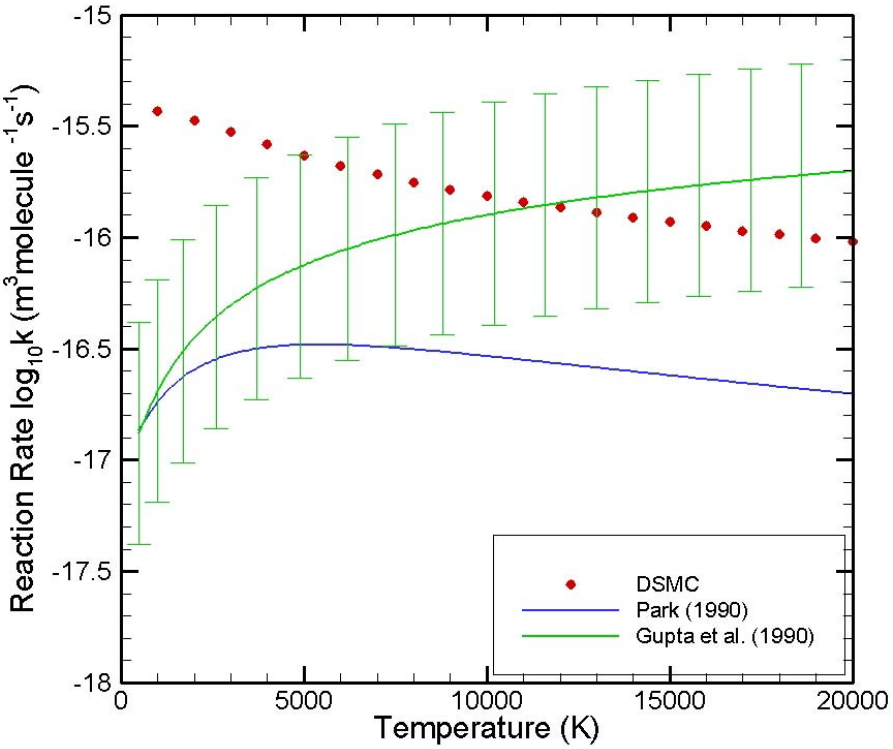

Figure 13. Oxygen/atomic-nitrogen exothermic exchange reaction: $O_2 + N \rightarrow NO + O$ **.**

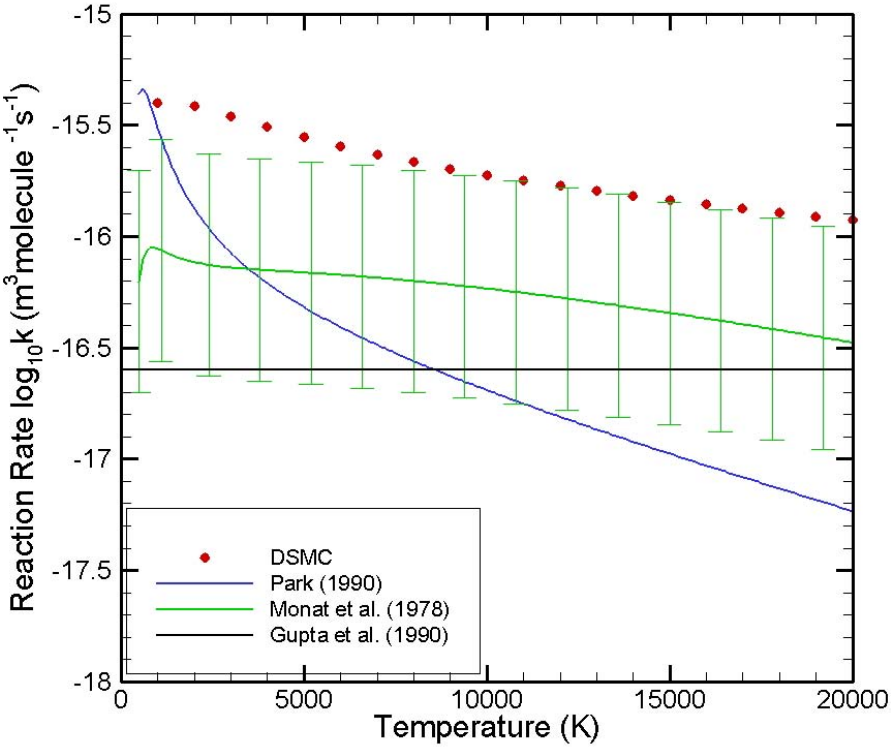

Figure 14. Nitric-oxide/atomic-nitrogen exothermic exchange reaction: $NO + N \rightarrow N_2 + O$ **.**

4.2 Non-Equilibrium Reaction Rates for Atmospheric Reactions

All cases examined so far involved gases in thermodynamic equilibrium. Although the ability of a chemistry model to reproduce equilibrium chemical reaction rates is a necessary condition, it is not sufficient to demonstrate that the method is capable to reproduce the correct reaction rates when the gas in not in thermodynamic equilibrium. Measured internal-energy-dependent cross sections of reactions between atmospheric species are extremely rare. Some systematic measurements and calculations exist for molecular hydrogen, where the cross section was found (Wadsworth and Wysong 1997) to be significantly affected by the distribution of energy among the reactant molecules. However, due to the relatively more important role of quantum effects in its chemistry, the behavior of hydrogen is expected to deviate from the behavior of heavier, and therefore more classical, atmospheric molecules.

4.2.1 Comparison of DSMC and Park's Model

Using the DSMC chemistry model-procedures, arbitrary non-equilibrium conditions can be simulated, and the effective reaction rate under conditions of non-equilibrium can be calculated. The calculation of non-equilibrium reaction rates with the DSMC code entails no differences in modeling since only collision-based molecular-level information is used.

For the study of non-equilibrium reaction rates, the test case selected is similar to the one used for equilibrium calculations, with the only difference being that the vibrational temperature of the gas is set independently from the temperature of the other modes. Thus, the gas is characterized by two temperatures, T_{tr} describing the translational and rotational modes, and T_{vib}, describing the vibrational mode. The energy states are distributed according to the Boltzmann distribution for the internal modes and the Maxwell distribution for the translational modes. These conditions simulate, to some degree, the state of the gas in a Navier-Stokes non-equilibrium calculation.

Figures 15 and 16 present non-equilibrium reaction rates for oxygen and nitrogen dissociation at four translational-rotational temperatures (3,000 K, 5,000 K, 10,000 K, and 15,000 K). Blue, green, red, and black in Figures 15 and 16 designate calculations at translational-rotational temperatures of 15,000 K, 10,000 K, 5,000 K, and 3,000 K, respectively. For each of these temperatures, the vibrational energy was distributed according to the harmonic oscillator model at a temperature that varied from 500 K to 15,000 K for oxygen and 1,000 K to 17,500 K for nitrogen. In both figures, the solid symbols represent the DSMC results. The solid lines in the figures represent Park's two-temperature reaction-rate model for non-equilibrium conditions, i.e., where the temperature in the Arrhenius rate suggested by Park is given by

$$T = T_{tr}^{q} T_{vib}^{1-q}, \tag{17}$$

with $q = 0.5$. The dashed lines present the measured equilibrium reaction rate at the average temperature (see Section 4.2.2). The solid and dashed lines do not intersect at the point of thermodynamic equilibrium, i.e., where $T_{tr} = T_{vib}$. This is a result of Park's suggested rates not fully conforming to the measured rates. Park's method yields good results at high temperatures

for both species. However, a discrepancy of several orders of magnitude appears for temperatures below 5,000 K.

The temperature regime of these figures is probably the most critical in modeling hypersonic flow fields since it mimics the conditions behind a shock layer (high translational temperature, low vibrational temperature). Assuming a typical high-altitude hypersonic flow field where the vibrational temperature is initially negligible, the flow will sweep the vibrational temperature regime from left to right in the figure. Thus, a poor estimate of the reaction rates in this initial temperature regime will yield lower dissociation of oxygen. The dissociation of oxygen is usually the first reaction that takes place in the flow field and is followed by the exchange reaction $N_2 + O \rightarrow NO + O$. Being a strong radiator, NO can be easily detected in the domain. Results based on underestimated dissociation reaction rates predicted by Navier-Stokes codes using Park's model yielded significantly lower (200 times) NO concentrations in the domain compared to flight measurements (Bose and Candler 1996).

Fitting the DSMC results by Park's Arrhenius-rate type of equation and using the temperature in Equation (17) with q as an adjustable parameter yields q values of 0.8 and 0.7 for oxygen and nitrogen, respectively. The resulting rates using these fittings appear in Figures 17 and 18 for oxygen and nitrogen. The color scheme in these figures follows the pattern of Figures 15 and 16. The non-equilibrium reaction rates using Park's model with the fitted values of q are in better agreement with the DSMC values, especially for temperatures less than 5,000 K. This indicates that a weaker dependence of the average temperature on the vibrational temperature may be more accurate and that multi-temperature effects on dissociation reaction rates may be smaller than initially anticipated, as previously suggested by Sharma et al. (1988).

Figures 19 and 20 present the rates for the $N_2 + O \rightarrow NO + N$ and $NO + O \rightarrow O_2 + N$ exchange reaction, respectively. Again, the color pattern of Figures 15 and 16 is followed. Park's model appears to be in agreement with the DSMC rates for near-equilibrium conditions although the discrepancy in the-lower vibrational-temperature regime observed for dissociation reactions is observed here as well. In the absence of non-equilibrium validation data, a comparison between two numerical models cannot produce unambiguous conclusions about the validity of either method. Further evidence, introduced by comparison to other theoretical models in Sections 4.2.3 -4.2.5, will allow for further conclusions to be drawn.

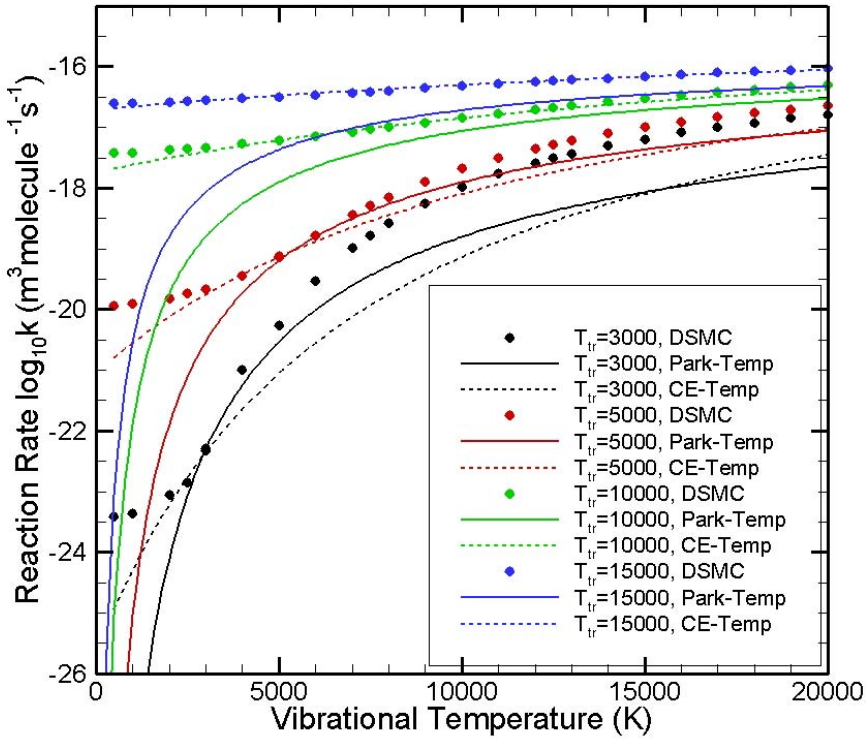

Figure 15. Oxygen dissociation. DSMC and Park's model.

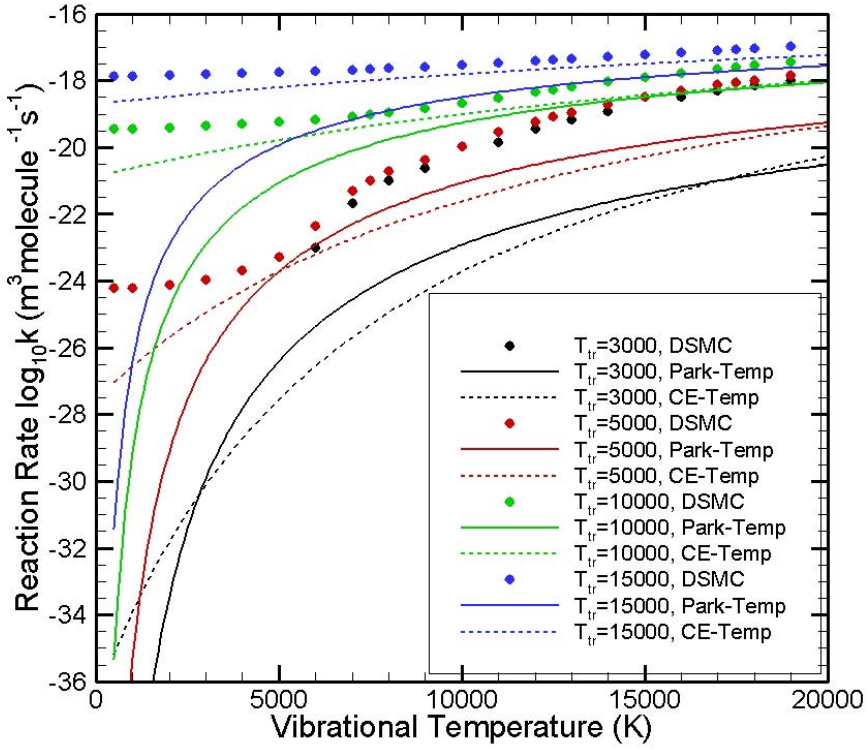

Figure 16. Nitrogen dissociation. DSMC and Park's model.

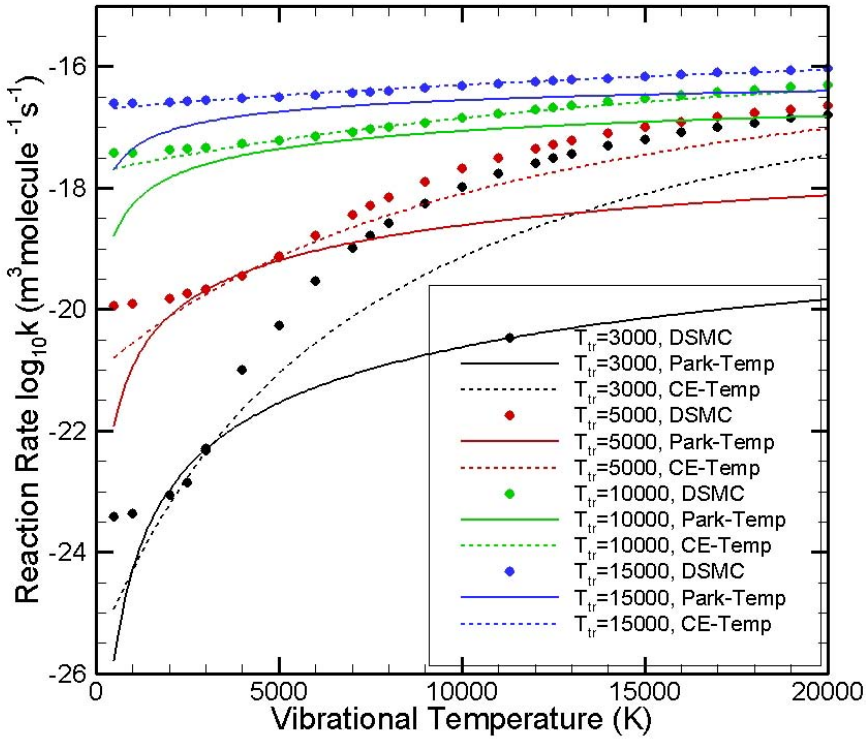

Figure 17. Oxygen dissociation. DSMC and Park's model fit using $q = 0.78$.

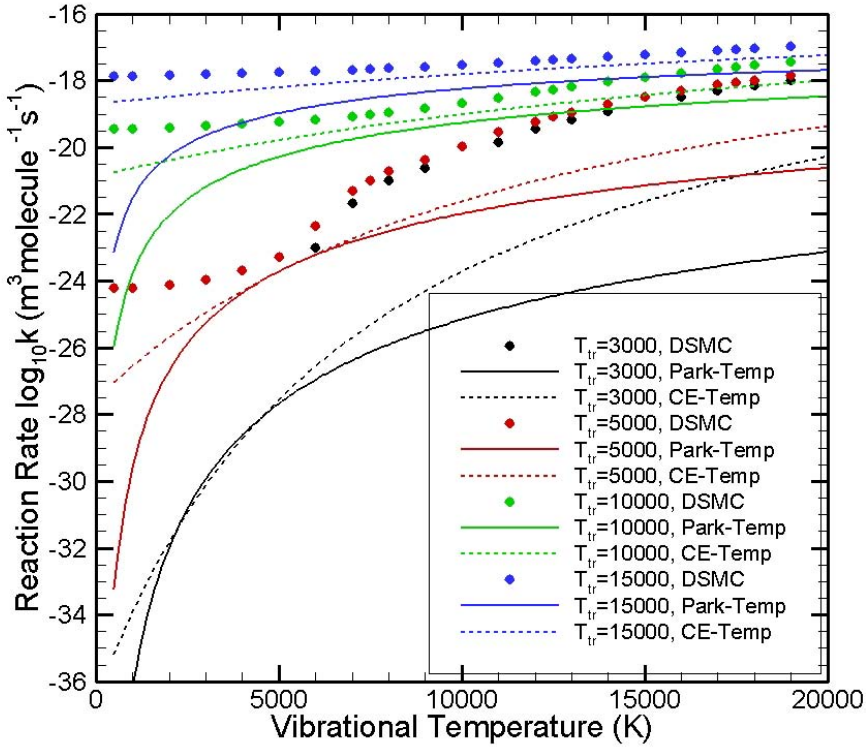

Figure 18. Nitrogen dissociation. DSMC and Park's model fit using $q = 0.7$.

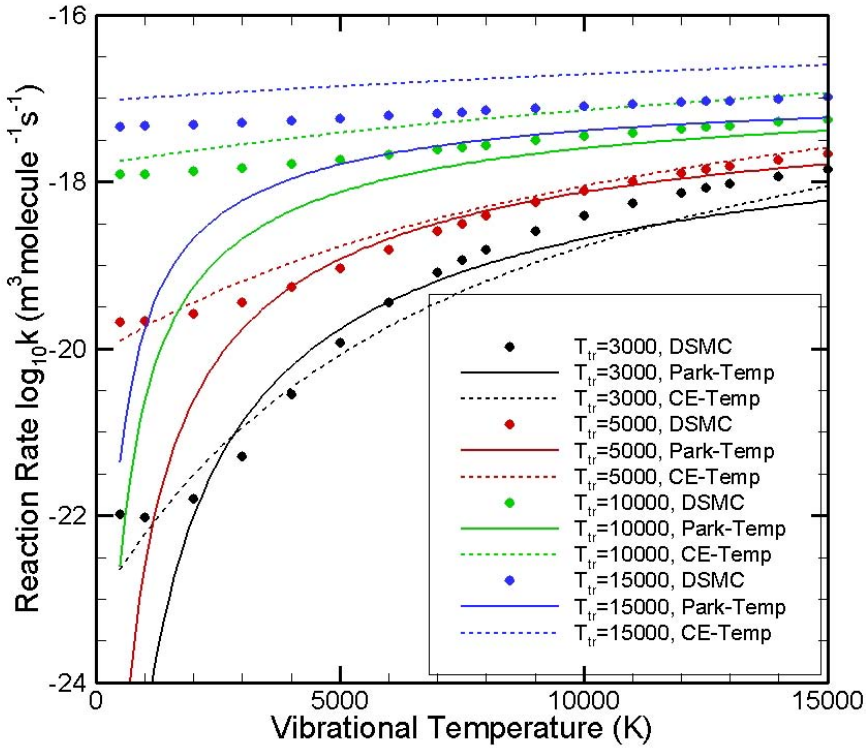

Figure 19. $N_2 + O \rightarrow NO + N$ **exchange reaction. DSMC and Park's model.**

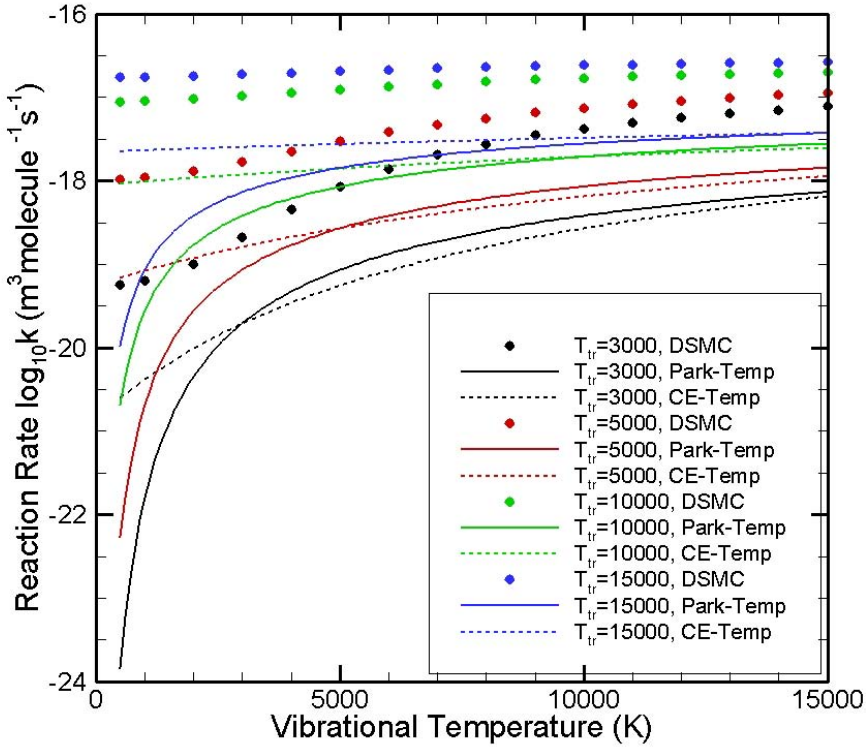

Figure 20. $NO + O \rightarrow O_2 + N$ **exchange reaction. DSMC and Park's model.**

4.2.2 Comparison of DSMC and Arrhenius Rates at the Average Temperature

For a gas not in a uniform steady state, the temperature T at any point is defined (Chapman and Cowling 1970) as that for which the same gas, when in uniform steady state at the same density, would have the same mean thermal energy per molecule. Thus, the Chapman-Enskog (CE) definition of temperature for a gas that is not in thermal equilibrium is

$$T = \frac{3T_{tr} + \zeta_{rot}T_{rot} + \zeta_{vib}T_{vib}}{3 + \zeta_{rot} + \zeta_{vib}}. \tag{18}$$

Equation (18) is an expression of the temperature as the average energy among all available internal energy modes. With this interpretation of temperature in terms of the average energy, the Arrhenius rates can provide an estimate of the non-equilibrium reaction rate in the absence of any other information. This interpretation of the Arrhenius reaction rate can also be treated as a limiting case since no preference is given to any particular mode in promoting a reaction rate.

In Figures 15-20, the dashed lines present the measured equilibrium reaction rate at the average temperature. For example, the dashed lines in Figures 15 and 16 are the Arrhenius rates of Johnston (1968) and Bortner (1969) for oxygen and nitrogen dissociation, respectively. The DSMC data have not been fitted to the measured equilibrium reaction rates, so the differences between the measured and DSMC rates are due to the differences in their predictions for equilibrium conditions (see Figures 1-14).

It is observed that, for high-temperature cases, this simple interpretation of the temperature in the Arrhenius rates as the average energy sufficiently captures non-equilibrium effects, resulting in reaction rates that match the DSMC rates. The agreement breaks down at lower vibrational temperatures, where the agreement is good only in the near-equilibrium regime.

The agreement between the DSMC non-equilibrium reaction rates and the Arrhenius rates using the CE definition of the average temperature is not a tautology because the DSMC rates are unaware of the macroscopic reaction rate. The agreement also cannot be considered a validation of the DSMC procedures. When replacing the equilibrium temperature in the Arrhenius rate (Equation (9)) with the CE definition of the average temperature (Equation (18)), it is implicitly assumed that the reaction rate is driven by the total available energy. This assumption is a good approximation of Bird's (2009) scheme at higher temperatures, where all energy modes have enough energy to overcome the reaction threshold. Therefore, this agreement could be considered a verification of the DSMC procedures.

The suggestion that reaction rates are mainly influenced by the total energy available in reactants ostensibly conflicts with the notion that chemical reactions, and in particular dissociation reactions, are strongly influenced by the energy content of the vibrational energy mode since strong evidence exists that individual reactions are significantly influenced by the energy configuration of the reactants. However, it appears that, for highly energetic collisions, the energy exchange that takes place during a collision may somewhat mask this effect. In fact, theory (Levine and Bernstein 1987) supported by experiments suggests that, while for low

collision energies the selective energy requirements can significantly influence the reaction rate, at higher collision energies the energy requirements become less restrictive. Thus, for high temperatures, the availability, or not, of sufficient total collision energy to overcome the energy barrier for the reaction to proceed appears to be strongly influencing the reaction probability.

4.2.3 Comparison of DSMC and Non-Equilibrium Reaction Models

Significant effort has been expended in attempts to express the dependence of the rate constant on the degree of vibrational excitation through the non-equilibrium factor

$$k(T_{tr},T_{vib}) = k(T)Z(T_{tr},T_{vib}), \tag{19}$$

where the subscripts *tr* and *vib* denote the translational and vibrational energy modes, respectively. Many theoretical and semi-empirical theories provide estimates for the non-equilibrium deviational parameter $Z(T_{tr},T_{vib})$. Some of these models make use of empirical or adjustable parameters that are estimated based on experimental data or quantum mechanical computations, and some require only microscopic information. In general, these models can be divided into two categories.

i) Intuitive models, such a Park's model examined in the previous section, aim at providing an estimate of non-equilibrium effects based on experimental observations.
ii) Theoretical models describe the physical processes using simple mechanisms that provide insight into the role of vibrational energy in promoting chemical reactions.

The existing intuitive and theoretical models for dissociation reactions are more advanced than those for exchange reactions. Both classes of models have been extensively reviewed in the literature (Chernyi et al. 2004, Pogosbekian et al. 2006).

One of the most general models based entirely on theoretical considerations is the Adiabatic Dissociation Model (ADM) of Smekhov et al. (in Chernyi et al. 2004). The model assumes that the energy states are distributed according to the Boltzmann distribution for the internal modes and the Maxwell distribution for the translational modes. The vibrational modes and the translational modes are each characterized by a single but distinct temperature. The model assumes that dissociation can occur from any vibrational level, including the ground state. However, the energy threshold is a function of the translational energy, compensating in this way for the intra-molecular energy transfer that can take place during a collision. The dissociation cross section is given by the Massey adiabatic parameter as $\sigma = \sigma_T \exp(-\xi)$, where σ_T is the total cross section and ξ is a function of the translational energy (Chernyi et al. 2004). The vibrational mode is described by the Morse anharmonic oscillator model.

Figures 21 and 22 present the DSMC and ADM results for oxygen and nitrogen dissociation. The ADM results are given by solid lines, where blue, green, red and black designate translational-rotational temperatures of 15,000 K, 10,000 K, 5,000 K, and 3,000 K, respectively. The ADM non-equilibrium rates have been calculated as deviations from the measured equilibrium rates of Johnston (1968) for oxygen and Bortner (1969) for nitrogen, which is how results would be obtained if these models were used in a Navier-Stokes code having knowledge of only the

measured equilibrium reaction rates. The dashed lines present the measured equilibrium reaction rates, where the equilibrium temperature is replaced with the CE temperature of Equation (18).

It is observed that the ADM model, especially for low temperatures, is in very good agreement with the DSMC calculated rates. The lack of agreement for the higher temperatures can be attributed to the harmonic oscillator model used in the DSMC model to describe the vibrational mode. The agreement for oxygen is better than that for nitrogen because the DSMC results are in better agreement with the measured rates used as the equilibrium rate for the ADM model.

Figures 23 and 24 present similar comparisons between DSMC and the oxygen dissociation models of Marrone and Treanor (M-T) (in Chernyi et al. 2004) and Macheret and Fridman (M-F) (in Chernyi et al. 2004), respectively. The Macheret-Fridman model uses two distinct dissociation mechanisms, one from the lower vibrational levels and another from the upper vibrational levels. The translational energy plays a critical role for dissociation from the lower vibrational levels. Dissociation occurs only for particular relative configurations of colliding molecules that minimize the energy barrier. The Macheret-Fridman model has been shown to produce deviations from the experimental data in excess of one order of magnitude, a behavior observed here in the low-vibrational-temperature regime. The Marrone-Treanor model uses a truncated harmonic oscillator to describe the vibrational mode and assumes that dissociation can occur from any vibrational state without distorting the Boltzmann distribution of molecules over vibrational levels. The Marrone-Treanor model contains a free parameter that must be estimated by comparison with experimental data or quantum mechanical calculations. According to Capitelli et al. (2000), this adjustable parameter has to be a function of the translational temperature and the vibrational level for the model to produce results in agreement with quantum mechanical calculations. Even in this case, and in harmony with the results of Figure 24, the Marrone-Treanor model was found to underpredict reaction rates for low vibrational temperatures. Both the Macheret-Fridman and Marrone-Treanor models are limited to vibrational temperatures lower than the translational-rotational temperature. The values for the adjustable parameters employed in both models are the ones suggested by Chernyi et al. (2004).

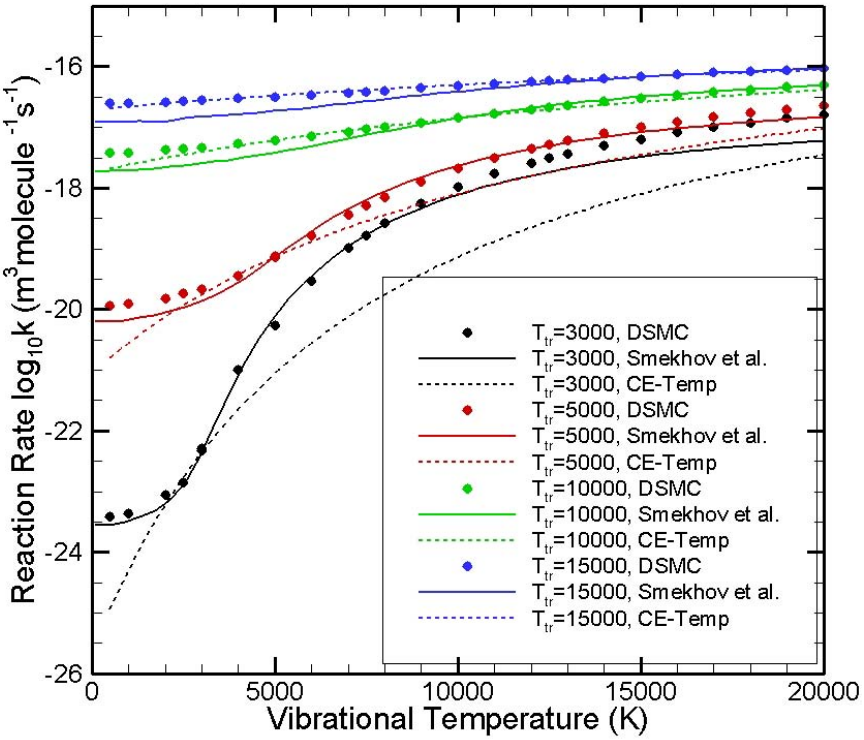

Figure 21. Oxygen dissociation. DSMC and ADM model.

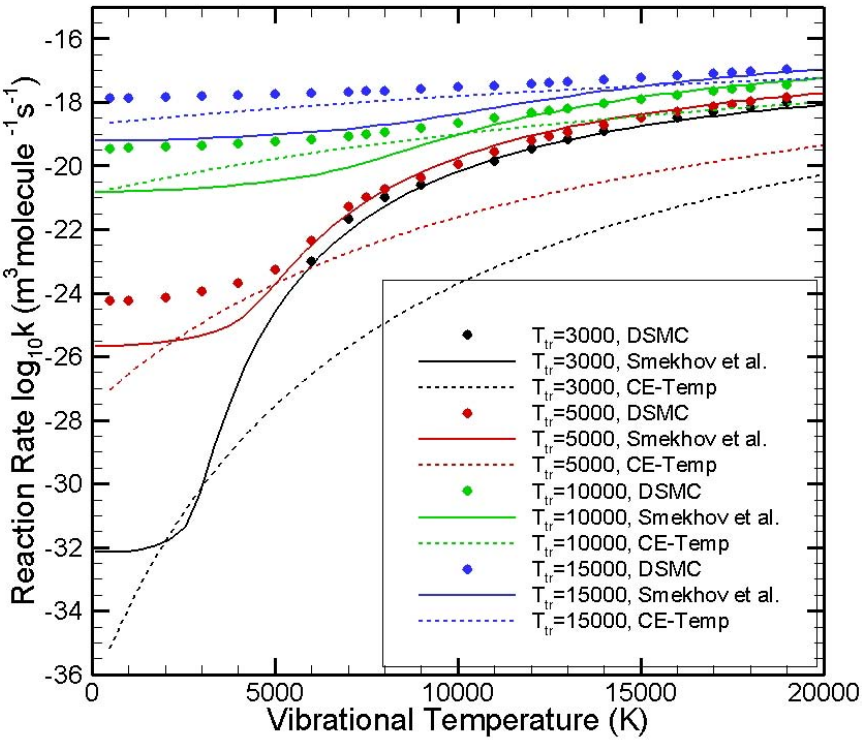

Figure 22. Nitrogen dissociation. DSMC and ADM model.

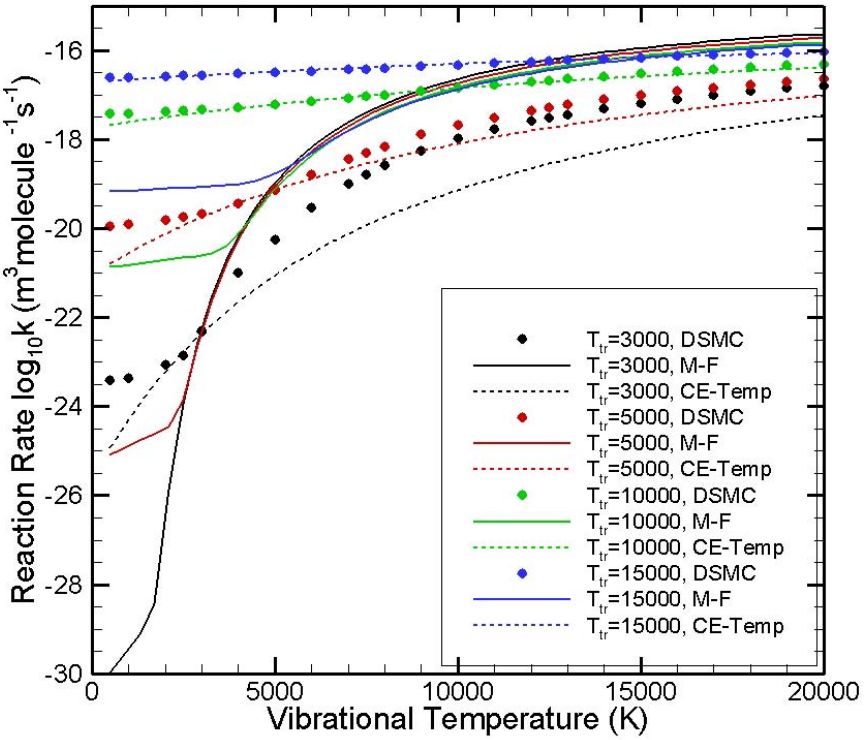

Figure 23. Oxygen dissociation. DSMC and Macheret-Fridman model.

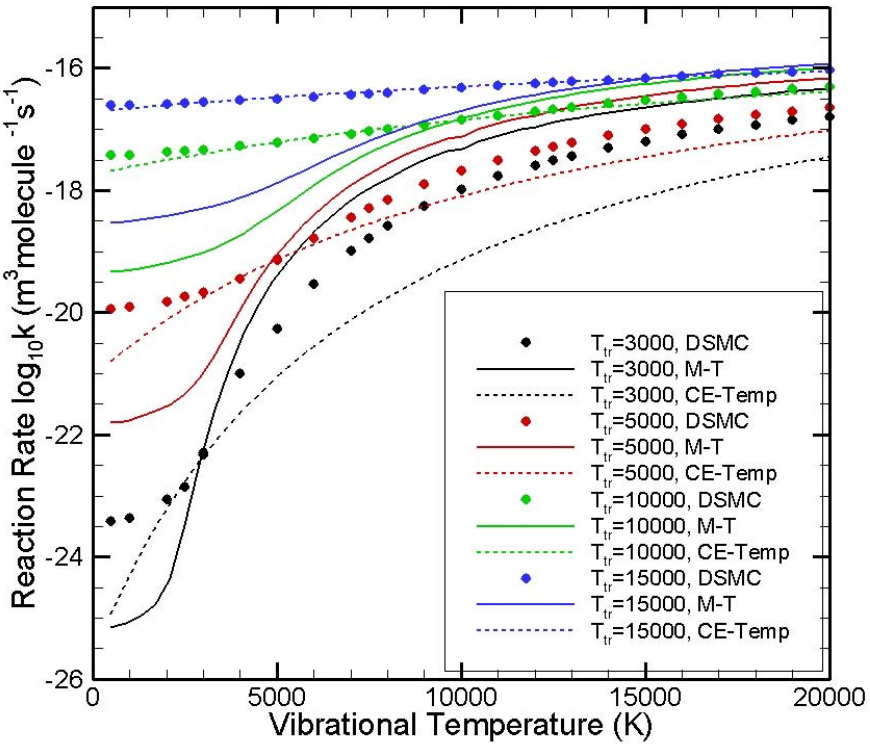

Figure 24. Oxygen dissociation. DSMC and Marrone-Treanor model.

The various theoretical models predict significantly different reaction rates at low vibrational temperatures. Evidently, the discrepancy between the predictions of the ADM, Macheret-Fridman, and Marrone-Treanor models is related to differences in allowing translational energy to promote dissociation reactions from low vibrational states.

Figures 25-28 present similar calculations for the exchange reactions of Equations (15) and (16). The DSMC non-equilibrium reaction rates here are compared to the models of Macheret and the α model (Chernyi et al. 2004). Both models are given by solid lines with color corresponding to the translational temperature. The α model assumes that vibrational energy plays a limited role in the reaction and only a fraction of it (α) participates in overcoming the energy threshold, whereas the translational energy is fully utilized in overcoming the energy threshold. Similarly, the Macheret model uses an adjustable parameter describing the fraction of vibrational energy that goes into the vibrational mode of the products in the reverse reaction, an expression of the principle of microscopic reversibility. The adjustable parameter of the Macheret model can be determined using experimental data. Parameters for a large number of exchange reactions are given in the literature (Chernyi et al. 2004). It should be noted that the Macheret model for exchange reactions is not the same as the one for dissociation reactions.

Figures 25 and 26 present the rates for the $N_2 + O \rightarrow NO + N$ exchange reaction using the Macheret model and the α model, respectively. For the second exchange reaction, $NO + O \rightarrow O_2 + N$, the rates for the Macheret and α models are presented in Figures 27 and 28, respectively. The Z factors used in all these comparisons were obtained from Chernyi et al. (2004), where the contributors of the models are also co-authors. The non-equilibrium reaction rates have thus been calculated as deviations from the measured equilibrium rates. In all these figures, the dashed lines present the equilibrium reaction rates at the average (CE) temperatures, and the solid lines present the non-equilibrium reaction rates as functions of measured equilibrium reaction rates.

Fairly good agreement between the DSMC rates and the theoretical models is achieved. Pogosbekian et al. (2006) compare quantum mechanical calculations for the $N_2 + O \rightarrow NO + N$ reaction to the Macheret model and observe good agreement for the regime of $T_{vib} = 10{,}000$ K and $T_{tr} \geq T_{vib}$. The α model results in higher reaction rates for low vibrational temperatures, which is also in agreement with the findings of Pogosbekian et al. (2006).

The difference between the theoretical models (non-equilibrium models and average temperature reaction rates) and the DSMC rates are due to the differences at equilibrium conditions since the DSMC rates have not been fitted to the equilibrium rates. To study how the DSMC non-equilibrium behavior compares with that of the theoretical models, the latter can be fitted to the DSMC equilibrium rates instead of to the measured equilibrium rates in cases where the two are not in agreement.

Figures 29 and 30 present the comparisons of Figures 26 and 28 of the α model to DSMC and average-temperature reaction rate, where the α model has been calibrated to the DSMC equilibrium reaction rate. Compared to Figures 26 and 28, it is observed that the α model, thus calibrated, produces non-equilibrium reaction rates that are in very good agreement with DSMC non-equilibrium rates. As pointed out earlier in this section, this agreement cannot be considered

a validation of either of the two models. However, based on the similarity of the two models, useful conclusions can be drawn about these models. The α fraction of the vibrational energy that participates in overcoming the energy threshold in addition to the translational energy could be related to the average vibrational energy that is disposed to the vibrational mode of the potentially formed products of the reaction. Chernyi et al. give values of $\alpha = 0.51$ and 0.94 for the reactions in Equations (15) and (16). Chernyi et al. also point out that for endothermic reactions α is expected to be in the interval $0.9 \le \alpha \le 1.0$. This may be the reason the agreement of this model with DSMC is better for the reaction in Equation (16) (Figure 30), where $\alpha = 0.94$, than for the reaction in Equation (15) (Figure 29), where $\alpha = 0.51$.

The agreement between DSMC and the α model in the low-vibrational-temperature regime is due to the fact that both models allow the translational energy alone to be used to overcome the energy threshold of the reaction, unlike Park's model, which predicts vanishing reaction rates as the vibrational temperature tends to zero. This difference between DSMC and Park's model is particularly important since in hypersonic reentry flow fields the free-stream vibrational temperature is typically negligible. Thus, any shock layer would necessarily go through the small vibrational temperature non-equilibrium regime presented on the left side of Figures 15-30.

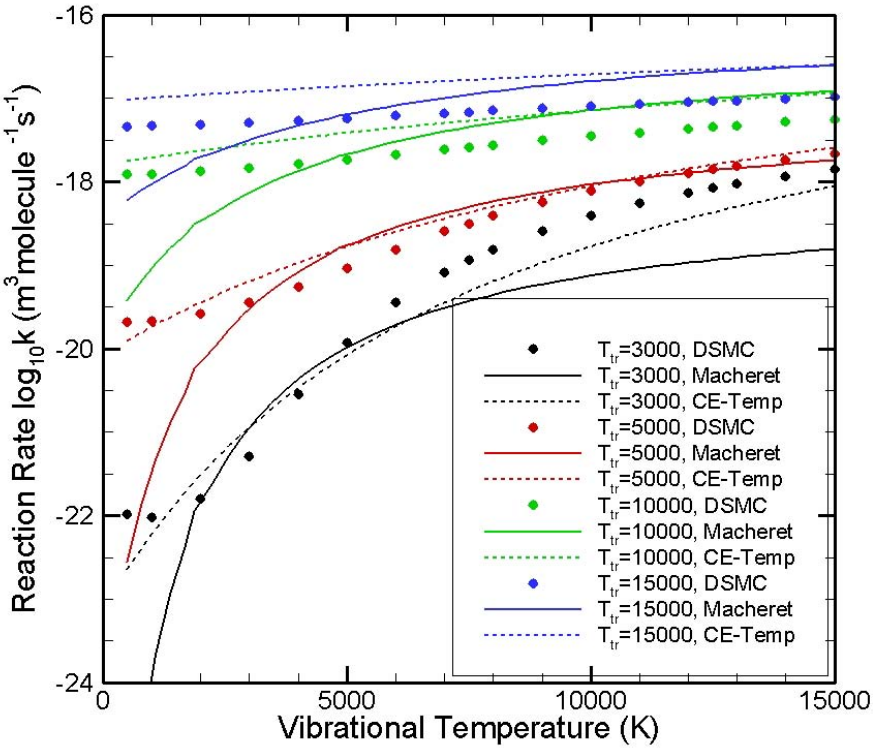

Figure 25. $N_2 + O \rightarrow NO + N$ **exchange reaction. DSMC and Macheret model.**

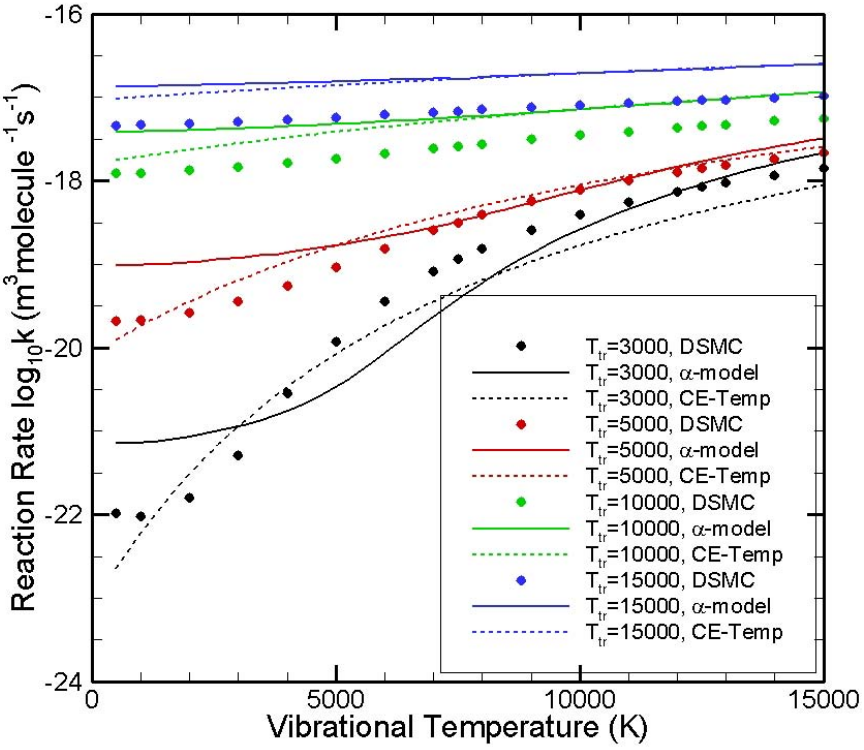

Figure 26. $N_2 + O \rightarrow NO + N$ **exchange reaction. DSMC and** α **model.**

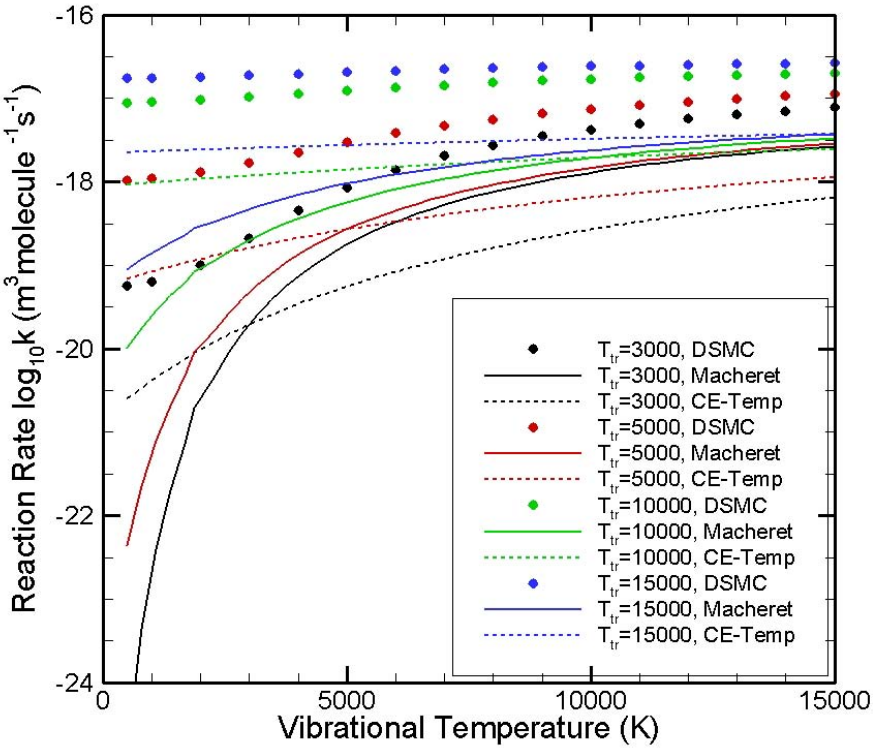

Figure 27. $NO + O \rightarrow O_2 + N$ **exchange reaction. DSMC and Macheret model.**

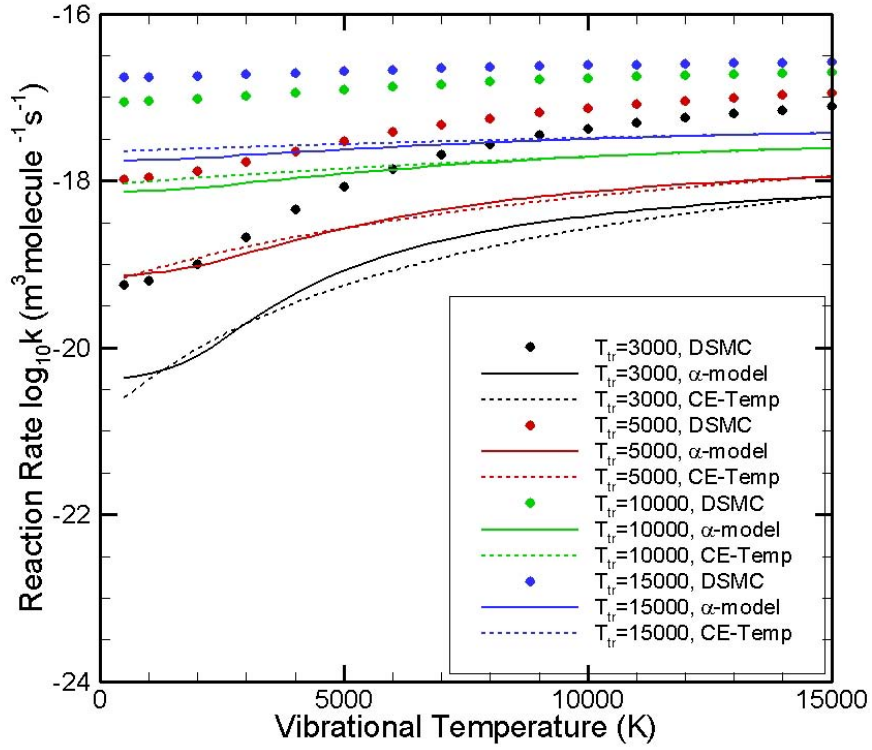

Figure 28. $NO + O \rightarrow O_2 + N$ **exchange reaction. DSMC and** α **model.**

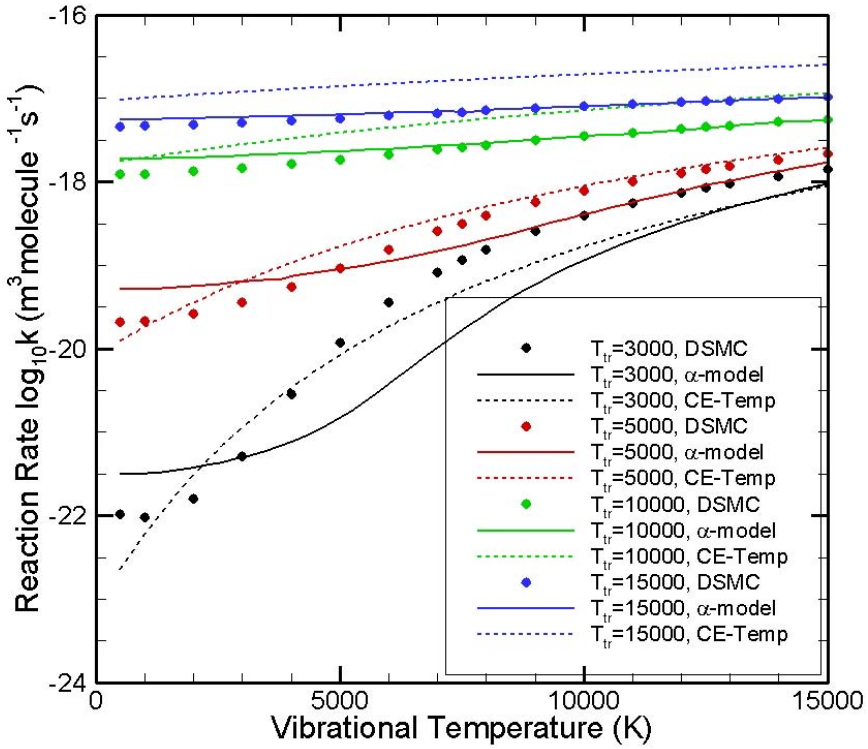

Figure 29. $N_2 + O \rightarrow NO + N$ **exchange reaction. DSMC and DSMC-calibrated** α **model.**

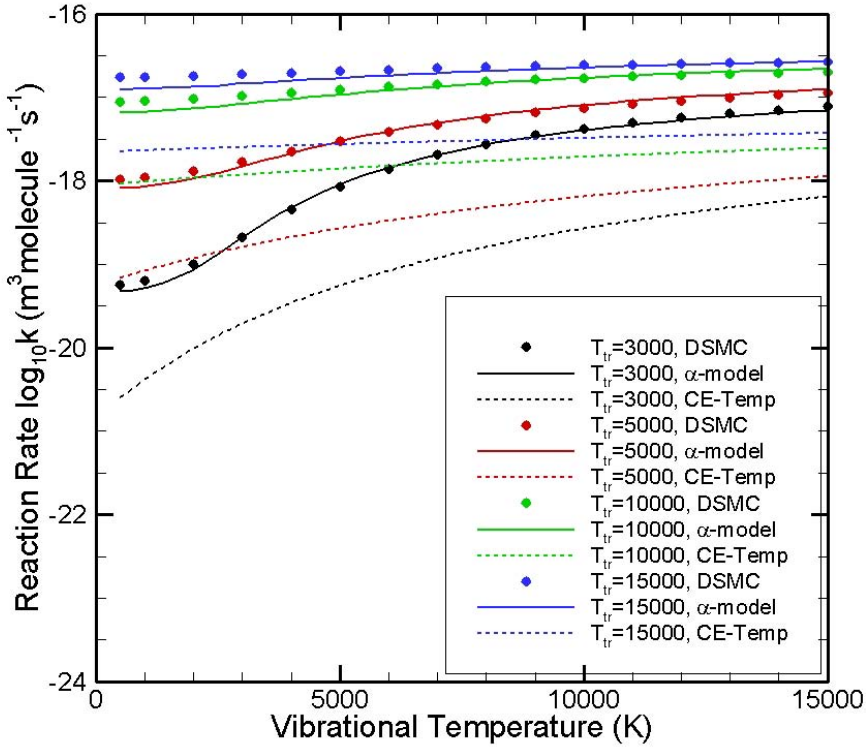

Figure 30. $NO + O \rightarrow O_2 + N$ **exchange reaction. DSMC and DSMC-calibrated** α **model.**

4.2.4 Comparison of DSMC and Measured Non-Equilibrium Reaction Rates

Very limited data are available for atmospheric species reaction rates under conditions of non-equilibrium. Sergievskaya et al. (1996) report a small number of dissociation reaction rates obtained from shock-tube measurements that involve atmospheric species.

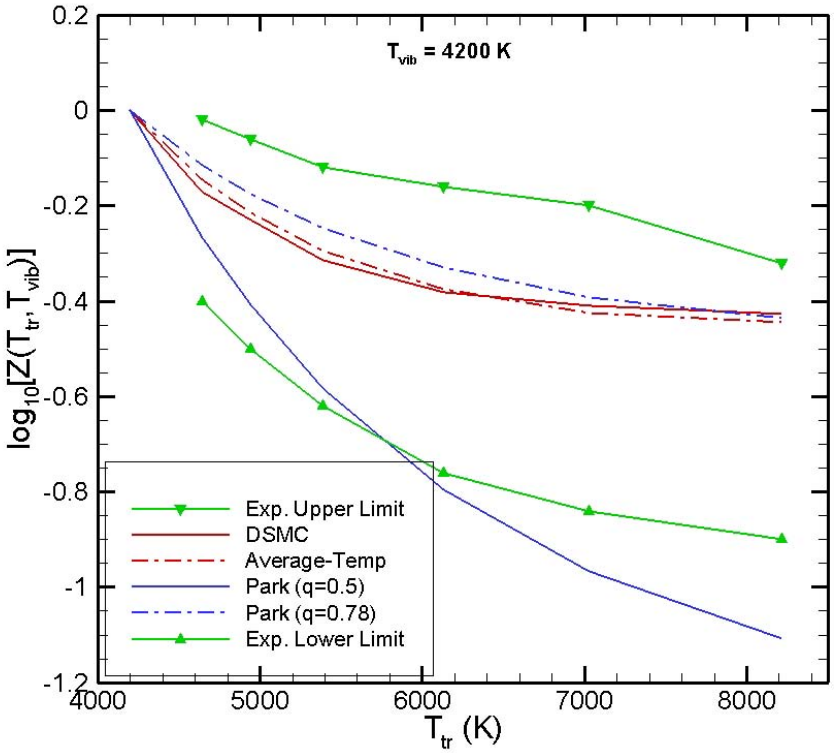

Figure 31. DSMC, Park, and measured non-equilibrium reaction rates.

Figure 31 presents measurements reported by Sergievskaya et al. (1996) for oxygen dissociation. The measurements presented with green lines in Figure 31 are upper and lower limits of the reaction rate. The spread of the measurements is somewhat below one order of magnitude. The vibrational temperature in these experiments was kept constant at 4,200 K while the translational and rotational temperatures were kept in equilibrium with each other. The non-equilibrium rates are presented in the form of the deviational parameter Z of Equation (19). Figure 31 also presents the ratio of the non-equilibrium to the equilibrium reaction rate as calculated by DSMC and Park's model using $q = 0.5$, as originally suggested by Park, and $q = 0.78$, as calculated in this work by fitting Park's model to DSMC data. The left side of the plot, where the blue and red lines intersect, is where the gas is in thermal equilibrium. As the translational temperature increases, the degree of non-equilibrium also increases.

As conditions depart from equilibrium, the DSMC predictions are bounded by the experimental results. Park's original model ($q = 0.5$) deviates from the measurements, when non-equilibrium becomes appreciable. However, adopting a factor of $q = 0.78$ for Park's model brings the non-equilibrium predictions in very good agreement with DSMC predictions.

Although less than one order of magnitude, the spread in the experimental measurements is significant, so an unequivocal assessment of the models cannot be made. However, the measured rates reproduce the trend observed in the previous section for highly non-equilibrium conditions, where the reaction rates were found to reach a plateau as a function of the translational temperature of the gas.

4.2.5 Comparison of DSMC and QCT Non-Equilibrium Reaction Rates

In the absence of measured data on cross sections for reactions between atmospheric species, advantage can be taken of Quasi-Classical Trajectory (QCT) calculations of molecular collisions, where the dependence of the cross section on the energy distribution can be estimated. One such effort by Bose and Candler (1996) reports internal-energy-dependent-rates for the endothermic exchange reaction between nitrogen and atomic oxygen, i.e., $N_2 + O \rightarrow NO + N$. This reaction is one of the most important chemical reactions in hypersonic flow fields because it is the main source of nitric oxide in the post-shock-layer flow field. This reaction has a low energy threshold that allows it to proceed in the presence of atomic oxygen, appearing due to the dissociation of molecular oxygen right behind a shock.

Bose and Candler (1996) present QCT calculations of this reaction and an analytical fit of the lowest ${}^3A'$ potential energy surface based on the Contracted Configuration Interaction (CCI) *ab initio* data. The chemical reaction rate from 3,000 K to 25,000 K is thus obtained. The calculated equilibrium reaction rates are found to be in good agreement with the measured rates, where data is available. Bose and Candler (1996) also present non-equilibrium reaction rates for particular vibrational energy states of molecular nitrogen.

Figure 32 presents a comparison between DSMC reaction rates and those of Bose and Candler (1996) for 7,000 K, 10,000 K, and 14,000 K. In these calculations, all nitrogen molecules were assumed to be at a particular vibrational level, whereas their translational and rotational energy was distributed according to the equilibrium distribution at the temperature of the calculation. The values are in fairly good agreement for low temperatures at low N_2 vibrational levels. However, as the temperature and the vibrational level increase, the discrepancy between the two models increases. The DSMC values appear to be plateauing around vibrational level 12, the energy-threshold level of Equation (13). If the condition of Equation (13) is replaced by

$$i_d \geq i \geq i_a \,, \tag{20}$$

suggesting that the energy level of the reactant molecule in a trial redistribution of energy should be between the energy thresholds of the exchange and dissociation reactions, the results of Figure 32 are replaced by those of Figure 33. In this case the results are in better agreement with the Bose and Candler (1996) calculations. Using the inequality in Equation (20) as the condition for an endothermic exchange reaction, the equilibrium reaction rate can be analytically given by

$$k(T) = \frac{2\sigma_{ref}}{\varepsilon\sqrt{\pi}} \left(\frac{T}{T_{ref}} \right)^{1-\omega} \left(\frac{2k_B T_{ref}}{m_r} \right)^{1/2} \left[\exp\left(-\frac{i_a \Theta_v}{T} \right) - \exp\left(-\frac{i_d \Theta_v}{T} \right) \right]. \tag{21}$$

The second term in the last bracket of Equation (21) becomes important only at high temperatures (greater than 15,000 K). The equilibrium reaction rate for the modified DSMC chemistry model (Equations (20) and (21)) is presented in Figure 34 and appears to be in very good agreement with the Bose and Candler (1996) reaction rate.

Source	**Reaction Rate** $\log_{10}(k)$	**Difference from Monat et al. (1978)**
Monat et al. (1978)	-19.7987	0%
Bose and Candler (1996)	-19.8048	2%
DSMC-Equation (13)	-20.1074	51%
DSMC-Equation (20)	-19.7987	16%

Table 1: Measured and calculated rates at 3,800 K for $N_2 + O \rightarrow NO + N$.

It is not clear whether this agreement indicates that replacing Equation (13) with Equation (20) provides a better representation of the actual chemical process since both results are numerical simulations of non-equilibrium conditions. As pointed out in Section 4.1.3, the experimental data for this reaction are very limited, and they are reliable only between 2,384-3,850 K. Comparing the reaction rates given by Monat et al. (1978), Bose and Candler (1996), and the DSMC models of Equations (13) and (20) at 3,800 K, the results in Table 1 are obtained. From these results, it is observed that the DSMC models are in good agreement with the measured rate. In fact, the DSMC model using the inequality in Equation (20) produces results lying within the reported 35% error margin of the measurements.

For the sake of completeness, the reaction rate applying the model of Equation (20) to the second reverse reaction, $NO + O \rightarrow O_2 + N$, is presented in Figure 35. Comparing Figure 33 to Figure 9, it is observed that modeling this reaction with the model of the inequality in Equation (20) results in higher reaction rates compared to the model of Equation (13). This effect is more pronounced for this reaction due to its lower energy threshold.

Adopting this model, the mechanism for the reverse, endothermic, exchange reactions needs to be revised to satisfy microscopic reversibility. Thus, the reverse reactions can be assumed to take place if the products of a hypothetical reaction have vibrational energy that lies in the regime described by the double inequality of Equation (20). The results of this model are given in Figures 36 and 37. In accord with the principle of microscopic reversibility and since the model of the inequality in Equation (20) results in higher reaction rates, so does the reverse reaction mechanism.

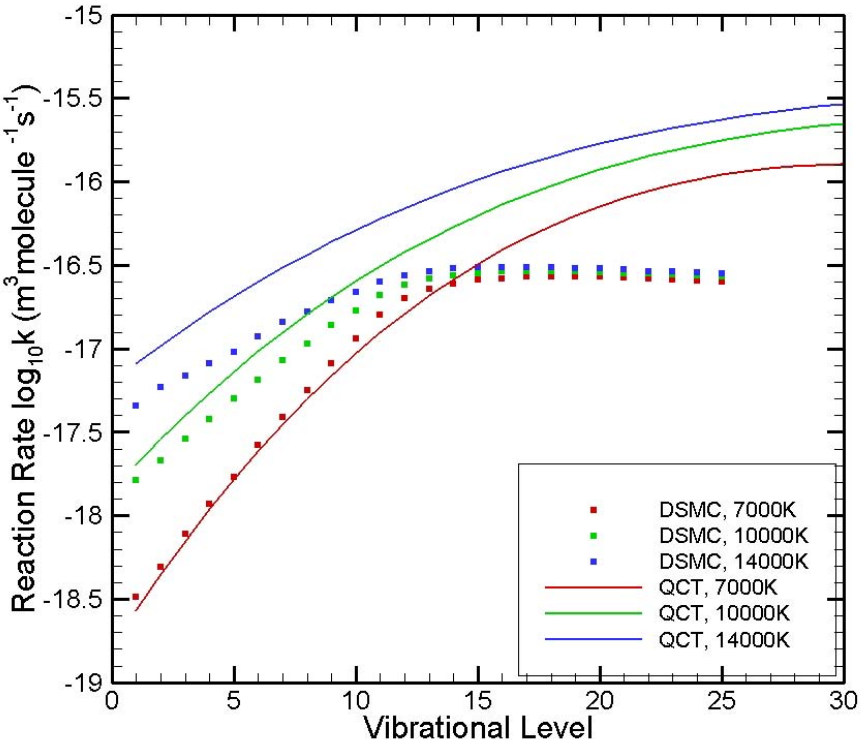

Figure 32. $N_2 + O \rightarrow NO + N$ **exchange reaction. DSMC-Eq. (13) and QCT results.**

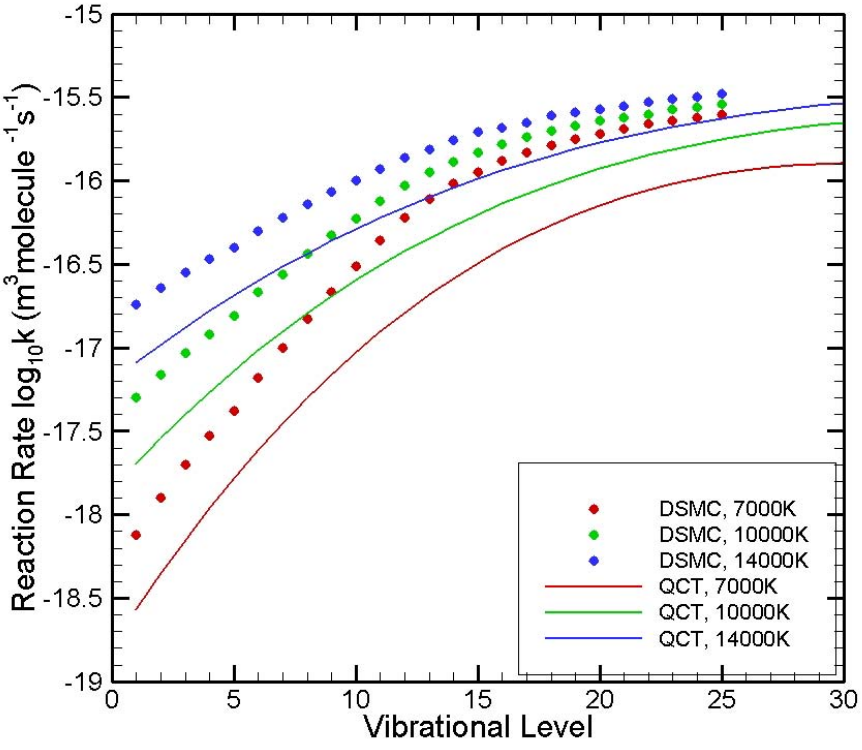

Figure 33. $N_2 + O \rightarrow NO + N$ **exchange reaction. DSMC-Eq. (20) and QCT results.**

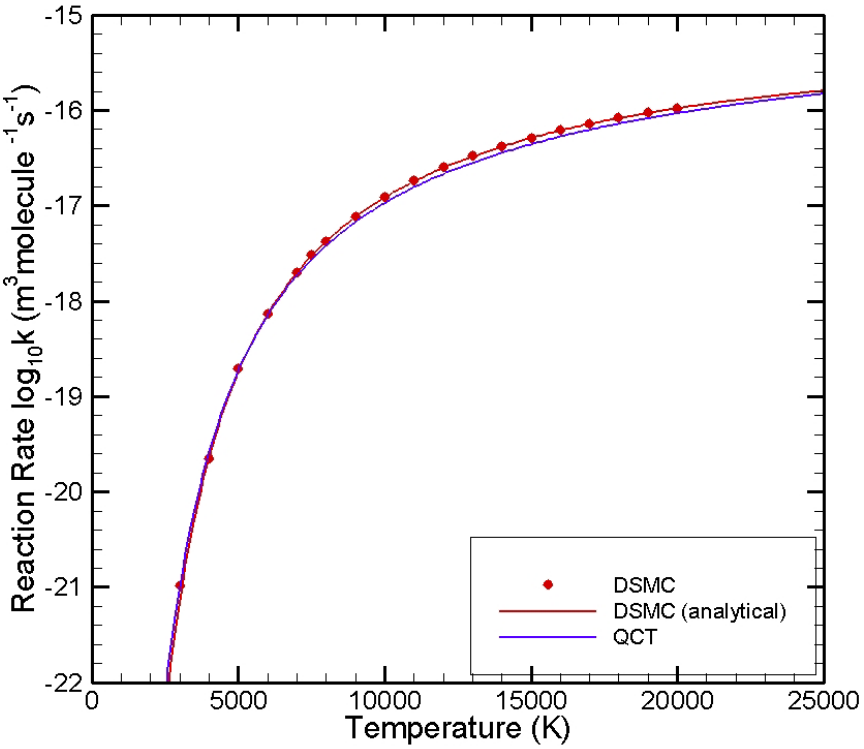

Figure 34. $N_2 + O \rightarrow NO + N$ **exchange reaction. DSMC-Eq. (20) and QCT equilibrium results.**

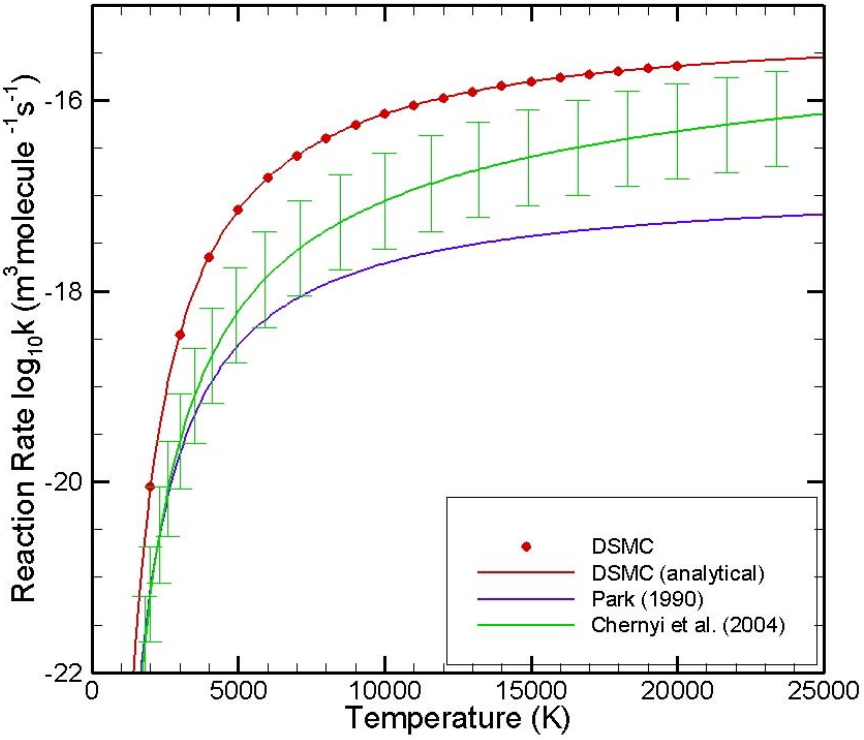

Figure 35. $NO + O \rightarrow O_2 + N$ **exchange reaction. DSMC-Eq. (20) and equilibrium results.**

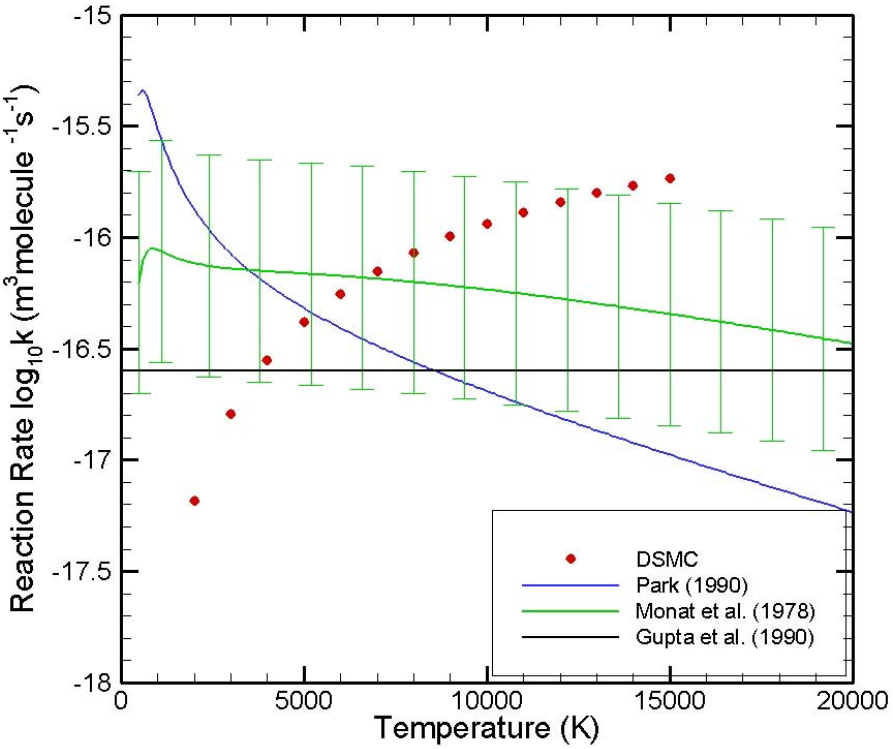

Figure 36. Nitric-oxide/atomic-nitrogen exothermic exchange reaction: $NO + N \rightarrow N_2 + O$**. DSMC-Eq. (20).**

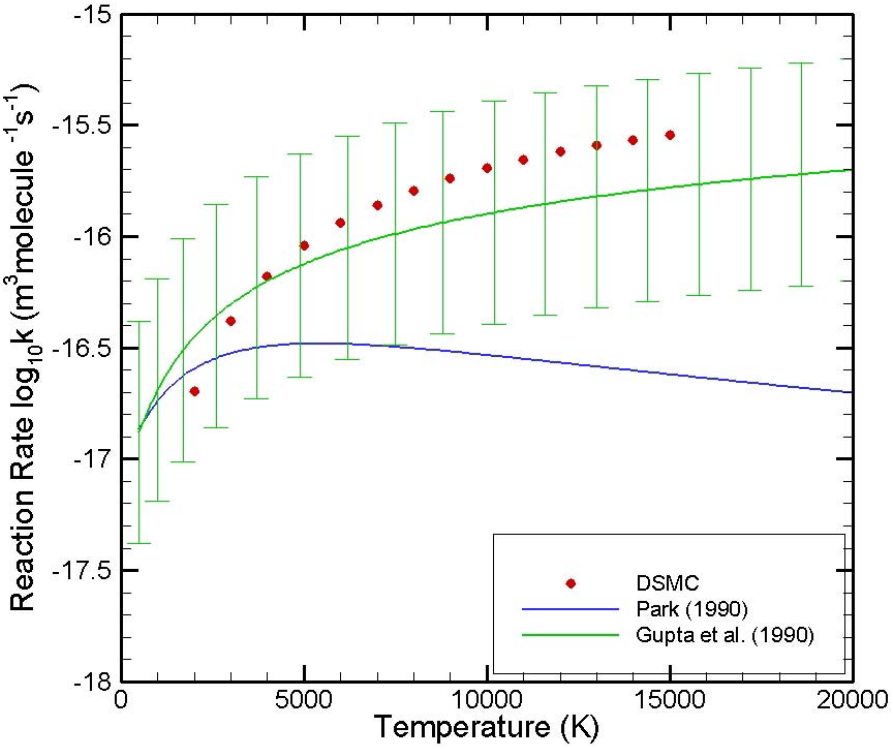

Figure 37. Oxygen/atomic-nitrogen exothermic exchange reaction: $O_2 + N \rightarrow NO + O$**. DSMC-Eq. (20).**

4.3 Combustion Reaction Rates

The ability of the DSMC procedures to cope with non-atmospheric species and lower than hypersonic-entry temperatures is very important to assess their ability to simulate chemical reactions mechanisms outside the typical regime of hypersonic aerodynamics and therefore to confirm their generality and applicability to other chemically reacting flows.

The traditional assumption that chemical processes are much faster than any other process (e.g., diffusion, heat conduction, and flow) does not break down only in the rather limited regime of hypersonic flow combustion. In many cases, chemical reactions take place on time scales which are comparable with those of flow and molecular transport. Thus, detailed information about individual elementary processes is required if transient processes like ignition and flame quenching in detonations need to be successfully modeled.

The hydrogen-oxygen combustion system was the first one used in detailed numerical studies of fuel oxidization. The reaction mechanism for H_2-O_2 combustion is much smaller than hydrocarbon oxidation, which makes it a good candidate for chemical kinetic modeling. Westbrook and Dryer (1984) present a hierarchical approach to combustion modeling. The strongly endothermic bimolecular reactions,

$$H + O_2 \rightarrow HO + O\,, \tag{22}$$

$$O + H_2 \rightarrow HO + H\,, \tag{23}$$

are the two most important chain-branching reactions, which are of fundamental importance in the ignition of H_2-O_2 mixtures as well as the oxidization of hydrocarbons, since they produce two radicals with the consumption of one. Therefore, these reactions influence important parameters of the combustion process, such as flame speeds. Unlike the chemical reactions in hypersonic flow fields that take place at temperatures in excess of 10,000 K, these reaction rates occur at more modest temperatures (300-3,000 K).

The hydrogen atoms in the system are introduced either at higher temperatures through hydrogen dissociation reactions or at lower temperatures through the reaction

$$H_2 + O_2 \rightarrow HO_2 + H\,. \tag{24}$$

Having a much lower dissociation threshold than oxygen, hydrogen dissociates first, allowing the reaction in Equation (22) to proceed. At temperatures high enough for oxygen to dissociate, the reaction in Equation (23) starts playing a larger role. Recombination may also play a significant role in removing some of the free radicals from the flow. The importance of recombination is reduced as the temperature of the flow increases.

Figures 38-40 present a comparison between measured reaction rates and the DSMC model of Section 3.1.4 for the reactions in Equations (22)-(24). DSMC simulations were not performed for these cases since the analytical expressions of the DSMC models were found to be in agreement with the numerical simulations for all cases examined (Figures 9 and 10).

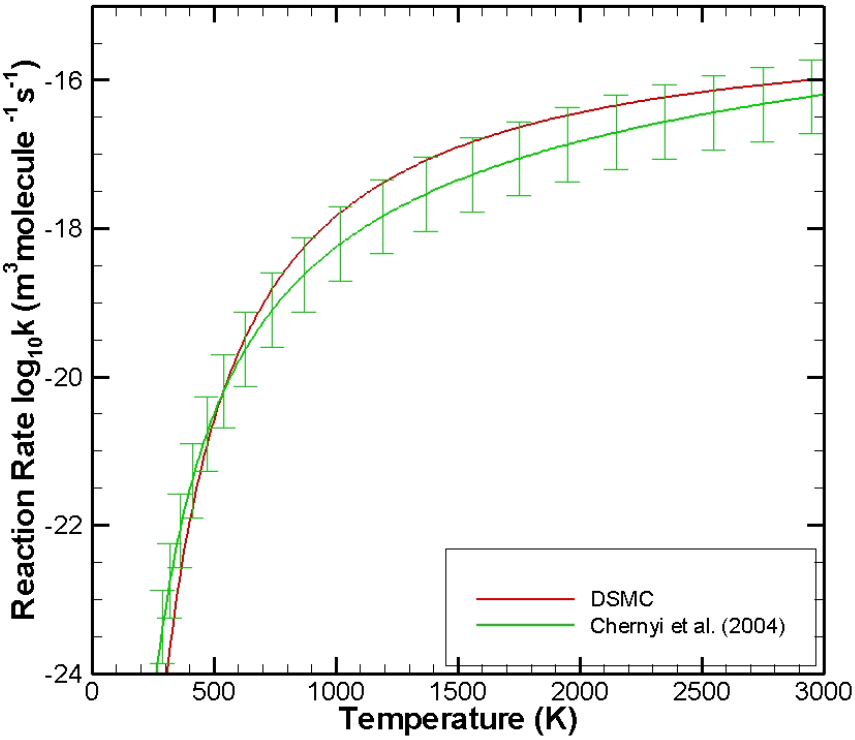

Figure 38. $H + O_2 \rightarrow HO + O$ **combustion reaction. DSMC and measured rates.**

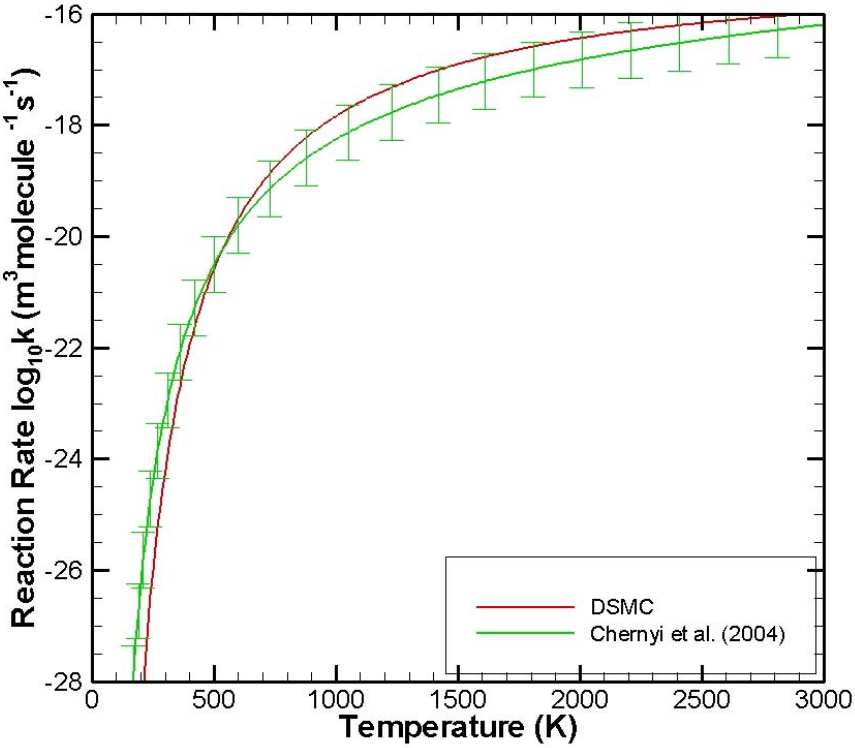

Figure 39. $O + H_2 \rightarrow HO + H$ **combustion reaction. DSMC and measured rates.**

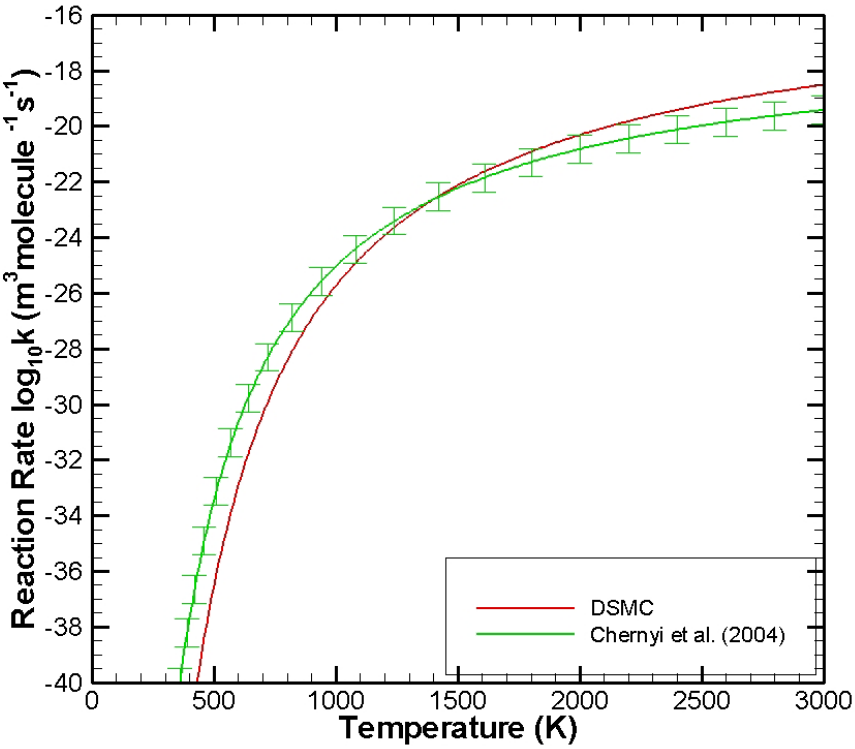

Figure 40. $H_2 + O_2 \rightarrow HO_2 + H$ **combustion reaction. DSMC and measured rates.**

Generally good agreement is observed for both these reaction rates. The agreement is encouraging because it demonstrates that the good agreement found for atmospheric species at high temperatures is also observed for non-atmospheric species at significantly lower temperatures.

4.4 Ionization Reaction Rates

Ionization reactions can be modeled in a manner similar to dissociation or exchange reactions if, depending on the type of the reaction, the vibrational mode in the chemistry model of Section 3.1 is replaced by the electronic mode. There is a direct analogy between dissociation or exchange reactions involving the vibrational states of molecules and ionization reactions involving electronic states. However, the close analogy stops at the description of electronic states. Not only are they more widely and unevenly spaced than vibrational states, but also the transitions between these states are subject to restrictive selection rules that make the use of tabulated data necessary.

To demonstrate the ability of the DSMC models to be extended to ionization reactions, a typical ionization reaction is herein studied. Hydrogen and hydrogen-like atoms have a particularly simple electronic structure that makes them good candidates for such a demonstration. Here, the ionization reaction studied is that of helium, with an ionization potential 24.587 eV:

$$He + He \rightarrow He + He^{+} + e^{-}. \tag{25}$$

This particular reaction was chosen not only because data on this reaction are available but also because it is similar to the ionization entry reaction $N + O \rightarrow NO^{+} + e^{-}$ for hypersonic flow fields. Equation (12) was used to calculate the resulting reaction rate. For the summation over all possible states, actual state-specific data were used (McQuarrie and Simon 1997) instead of the approximate model of Balmer (Herzberg 1939).

The model of Massey (in Chernyi et al. 2004) provides an estimate of the upper limit for the cross section and ionization rate in the sense that, like the DSMC model, selection rules have not been included in the model. Unlike the DSMC model, the model of Massey uses information on the interaction potential, a quantity that DSMC approximates using kinetic theory considerations.

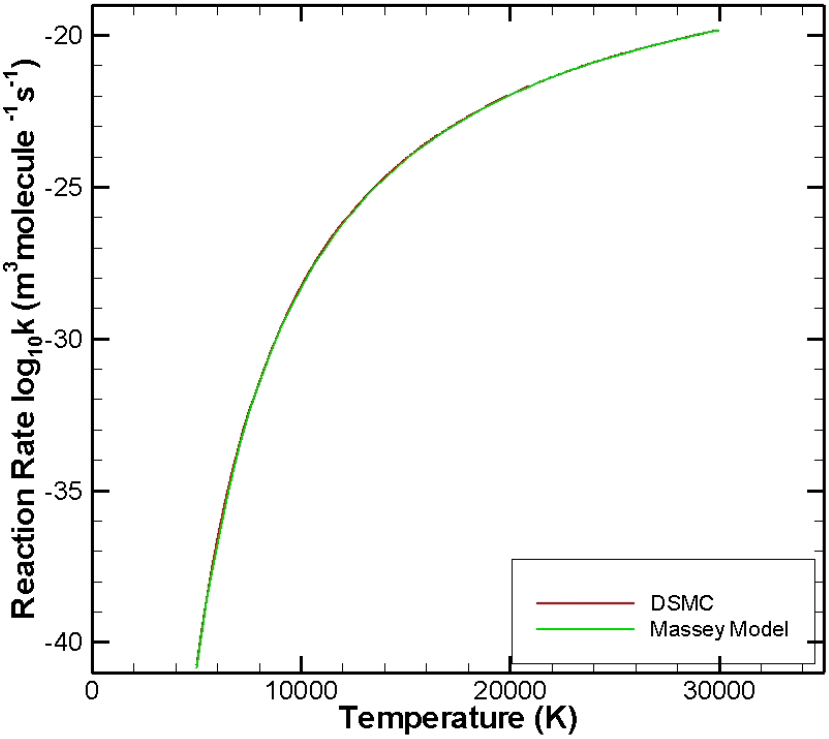

Figure 41. Helium ionization: $He + He \rightarrow He + He^{+} + e^{-}$. DSMC and Massey model.

Figure 41 presents a comparison between the Massey model and DSMC. The two models are in excellent agreement, which provides a verification of the DSMC procedures. Both, the DSMC and Massey models provide an upper estimate for the ionization rate since they are based solely on energetics and no selection rules have been implemented. Such selection rules may limit transitions only between neighboring states, i.e., where the quantum number changes by unity. However, such selection rules can straightforwardly be implemented in DSMC models.

Due to the lack of analytical descriptions or models for the electronic states and selection rules, implementing ionization mechanisms in DSMC is significantly more labor-intensive than for dissociation and exchange reactions. The electronic states of simple hydrogen-like atoms are given fairly accurately by the Balmer series (Herzberg 1939). For other more complicated molecules, the actual, state-specific data and transition selection rules must be implemented.

Although this may appear to be an overwhelming task, for non-equilibrium simulations this approach may be preferable since no information on cross-sections is available.

The advantage of using DSMC mechanisms in comparison to cross-section data becomes clearer when considering that DSMC models can also deal with the ionization of excited atoms or molecules, a frequently occurring mechanism in non-equilibrium plasmas, without any additional information. If cross-section data were used, then a very large database of all possible transitions would have to be created.

5. CONCLUSIONS

A set of recently proposed procedures to model chemical reactions within the context of the DSMC method has been implemented, verified, and validated. The new model, unlike all other DSMC chemical-reaction models available, does not rely on measured macroscopic reaction rates to calibrate adjustable parameters. Instead, it makes use of the principles of microscopic reversibility and molecular-level energy exchange to predict the probability of a chemical reaction occurring during a collision between two molecules. Based solely on molecular properties and collision energetics, the model cannot account for quantum mechanical effects applying to transitions between energy states.

Through a series of comparisons, it was established that the DSMC models can produce reaction rates in fairly good agreement with the best available measured or extrapolated reaction rates. The experimental uncertainty of the measurements and the idealizing assumptions of the calculations do not allow for an unequivocal assessment of the models in question through these comparisons. However, the discrepancies between the currently most reliable reaction-rate data and the DSMC predictions appear to be always within one order of magnitude. This level of agreement between the DSMC models and measured and calculated rates is a source of optimism concerning the ability of the method to provide predictions of non-equilibrium reaction rates between these species.

For non-equilibrium conditions, Park's model, the predominant chemical reaction model used in Navier-Stokes calculations, produces a non-physical behavior for low vibrational temperatures. The DSMC model is found to be in very good qualitative and quantitative agreement with theoretical predictions and well within the accuracy of measured non-equilibrium reaction-rate predictions. In fact, the DSMC results indicate that, in agreement with theoretical predictions and experimental observations, the selectivity of a reaction rate on the reactant energy is minimized as the total collision energy increases.

Extension of the DSMC procedures to reactions typically found in combustion indicates that the same level of agreement can be achieved. This finding is particularly important since it indicates that the DSMC model is applicable not only to atmospheric reactions and reentry level temperatures but also to combustion reactions at lower temperatures. The DSMC model could be of value to the study of combustions systems when thermal non-equilibrium is observed in the flow or when chemical reaction rates cannot be reliably measured.

It is often advocated that the inclusion of measured or calculated reaction cross sections would form the ultimate DSMC chemistry model. Even if that were possible, the end result would probably not be correct. DSMC procedures are phenomenological in nature and attempt to mimic the actual procedures so as to reproduce some critical flow parameters. For example, the collision cross section predicted by the VSS model is clearly not the actual collision probability of two molecules but rather an estimated collision probability that leads to the correct viscosity and diffusivity. Thus, using the "actual" reaction cross sections may not necessarily lead to correct reaction rates. Rather, as the model procedures investigated herein suggest, a procedure consistent with the fundamental assumptions of the method that mimics core features of the microscopic process may lead to the correct macroscopically observable flow features.

Currently, the ability to simulate upper-atmosphere hypersonic flows and environments is hampered by using chemical-reaction-rate models of unknown accuracy that introduce unquantifiable errors into calculations. This new DSMC approach based on molecule-level processes appears to lead to a truly predictive capability for estimating chemical-reaction rates at equilibrium as well as non-equilibrium conditions that does not rely on measured equilibrium rates.

The non-equilibrium, high-temperature chemical-reaction rates computed by DSMC can be incorporated into new non-equilibrium reaction-rate models for Navier-Stokes codes. The resulting chemical-reaction-rate models will enable Navier-Stokes codes to reproduce certain non-equilibrium effects currently available only to DSMC codes. Further work could establish a set of chemical reactions and chemical reaction rates used by both the DSMC and Navier-Stokes codes, allowing for a consistent study of reentry processes with chemistry models of known accuracy and applicability.

6. APPENDIX: DSMC AND THE LARSEN-BORGNAKKE MODEL

The form of the Larsen-Borgnakke energy-exchange model used for the division of energy between the translational and internal modes of a polyatomic molecule participating in a collision is the General Larsen-Borgnakke (GLB) model of Bird. The GLB model includes all previous cases of rotational and vibrational energy exchange as special cases. The application of the model is demonstrated with an example. Assume that two polyatomic molecules collide with an average number of degrees of freedom $\zeta_{ave} = (5/2-\omega)+1/2[\zeta_{rot,1}+\zeta_{rot,2}+\sum\zeta_{vib,1}+\sum\zeta_{vib,2}]$.

The translational mode contributes $(5/2-\omega)$ degrees of freedom, and the subscripts *rot* and *vib* stand for the rotational and vibrational degrees of freedom contributed by each molecule, denoted by co-subscripts *1* and *2*. The energy exchange between the two molecule simulators is performed by a succession of redistributions, each one involving a particular internal mode of one of the colliding molecules and the translational mode.

The vibrational collision number has the form given by Millikan and White (Bird 1994):

$$Z_{\text{vib}} = \left(C_1/T^{\omega}\right)\exp\left[C_2/T^{1/3}\right]. \tag{26}$$

For nitrogen, Millikan and White suggest parameter values of $C_1 = 9.1$ and $C_2 = 220.0$, where the temperature T is in K.

Bird (2009) suggests using a vibrational relaxation number based on collision-pair properties instead of using the macroscopic temperature of the gas or the computational cell as in Equation (26). Thus, the vibrational relaxation number can be written as

$$Z_{vib} = \left(\frac{\Theta_d}{T}\right)^{\omega}\left[Z_{ref}\left(\frac{\Theta_d}{T_{ref}}\right)^{-\omega}\right]^{\left[\left(\frac{\Theta_d}{T}\right)^{-1/3}-1\right]\Big/\left[\left(\frac{\Theta_d}{T_{ref}}\right)^{-1/3}-1\right]}, \tag{27}$$

where Θ_d is the characteristic temperature of dissociation, and Z_{ref} is the relaxation number at temperature T_{ref}.

The temperature T is calculated at the collision level as

$$T_{coll} = i_{\max}\Theta_v/(7/2-\omega), \text{ where } i_{\max} = \text{int}[E_c/k_B\Theta_v]. \tag{28}$$

Equations (27) and (28) ensure that equilibration is achieved by using only collision-pair information.

The relaxation rate is controlled by allowing a fraction $\phi = 1/Z$ of collisions to exchange energy. Typically, ζ and Z are specified separately for each mode of internal energy, and the GLB model is applied serially when multiple modes are present (e.g., vibration and rotation). An important simplification of Equations (3) and (4) is obtained for the special case where ζ =2,

i.e., for the internal modes of diatomic molecules. In this case, the last term in Equations (1) and (2) disappears. This allows for the inverse distribution to be calculated and subsequently an explicit function for E_i to be calculated as a function of a random number. More details about this model are given by Bird (1994).

The rotational energy modes of a polyatomic molecule generally have many closely spaced energy states relative to translational energies and hence are fully excited. Thus, a continuous classical description is adequate. The rigid-rotor model is appropriate for linear molecules and in particular for diatomic molecules. In this model, molecules carry two rotational degrees of freedom, so $\zeta_{\text{rot}} = 2$ in the GLB model. The equation of Parker is used to prescribe the rotational collision number Z_{rot} (Bird 1994):

$$Z_{\text{rot}} = \frac{Z_{\text{rot}}^{\infty}}{1+\left(\pi^{3/2}/2\right)\left(T^*/T_{\text{tr}}\right)^{1/2}+\left(\pi+\pi^2/4\right)\left(T^*/T_{\text{tr}}\right)}, \tag{29}$$

where Z_{rot}^{∞} and T^* are constants for the given gas and T_{tr} is the translational temperature, which corresponds to the total translational energy E_t in the GLB model. For nitrogen, Parker suggests $Z_{\text{rot}}^{\infty} = 15.7$ and $T^* = 80.0$ K, whereas Lordi and Mates suggest $Z_{\text{rot}}^{\infty} = 23.0$ and $T^* = 91.5$ K (Bird 1994). For temperatures in the range of 100-1,000 K, both sets of values produce Z_{rot} values in the range of 2-10 (the Parker values are slightly smaller). It is noted that a value of $Z_{\text{rot}} = 1$ allows exchange of rotational and translational energy during every collision.

To calculate the energy of the rotational mode of molecule i ($i = 1, 2$), the following steps are followed. The probability of energy exchange between the translational mode and the rotational mode $\phi = 1/Z$ is calculated using Equation (29). If the probability is found to be greater than a random number (accept-reject technique), the energy content of this mode is left unchanged, and the procedure continues with the remaining available modes. If the probability is found to be less than a random number, the mode is approved for energy exchange, and a random part E_i of the available energy E_c is selected as a candidate energy for the mode. The available energy E_c is the sum of the energy of the translational mode and the internal mode in question, i.e., the rotational mode of the second molecule in this example. The probability of this event is estimated using Equation (4) setting $\zeta = \zeta_{rot,i}$. Again, an accept-reject technique is applied and if the energy E_i is accepted, the procedure continues with the following mode. If not, a new fraction of E_c is selected, and the accept-reject continues until an acceptable energy configuration is selected.

This procedure continues for all modes of both molecules, and whatever energy is left is assigned to the translational mode. At first, this procedure may appear to favor the first modes examined in the serial application of the GLB model. However, this is not the case. The random selection of candidate energy levels in conjunction with the application of an accept-reject technique ensures that all modes, regardless of the order they are examined, have an equal chance of accessing all the available energy states. This procedure can be applied to all energy modes for which a continuous description can be considered as adequate.

Although for very-high-temperature hypersonic flow the vibrational mode may have a continuum distribution, in most cases in subsonic flows, it does *not*. The GLB model, therefore, is applied as for the continuous modes with the exception that the random selection of the potential energy content of a vibrational mode is made using Equation (5), i.e., by randomly selecting an integer energy state i from 0 to the maximum allowable energy state $E_c/(k_B\Theta_v)$. Then the rest of the model is applied in the same way regardless of how the energy of the state was calculated.

7. REFERENCES

G. A. Bird, "Simulation of Multi-Dimensional and Chemically Reactive Flows", *Rarefied Gas Dynamics*, Ed. R. Campargue, CEA, Paris, pp. 365-388, 1979.

G. A. Bird, *Molecular Dynamics and the Direct Simulation of Gas Flows*, Oxford University Press, Oxford, UK, 1994.

G. A. Bird, "A Comparison of Collision Energy-based and Temperature-based Procedures in DSMC", *Rarefied Gas Dynamics, 26th Symposium*, **1084**, Ed. T. Abe, American Institute of Physics, pp. 245-250, 2009.

G. A. Bird, M. A. Gallis, J. R. Torczynski, and D. J. Rader, "Accuracy and Efficiency of the Sophisticated DSMC Algorithm for Simulating Non-Continuum Gas Flows", *Physics of Fluids*, **21**, 017103, 2009.

M. H. Bortner, "A Review of Rate Constants of Selected Reactions of Interest in Re-Entry Flow Fields in Atmosphere", NBS TN 484, 1969.

D. Bose and G. V. Candler, Thermal Rate Constants of the $N_2 + O \rightarrow NO + N$ Reaction Using *Ab Initio* ${}^3A"$ and ${}^3A'$ Potential Energy Surfaces, *Journal of Chemical Physics*, **104**, (8), pp. 2825-2833, 1996.

M. Capitelli, F. Esposito, E. V. Kustova, and E. A. Nagnibeda, "Rate Coefficients for the Reactions N2(i)+N=3N: A Comparison of Trajectory Calculations and the Treanor-Marrone Model", *Chemical Physics Letters*, **330**, pp. 207-211, 2000.

S. Chapman and T. G. Cowling, *The Mathematical Theory of Non-Uniform Gases*, Cambridge University Press, Cambridge, UK, 1970.

G. G. Chernyi, S. A. Losev, S. O. Macheret, and B. V. Potapkin, "Physical and Chemical Processes in Gas Dynamics", Vol. I: Cross Sections and Rate Constants, *Progress in Aeronautics and Astronautics*, **197**, 2004.

R. A. Dressler, *Chemical Dynamics in Extreme Environments*, World Scientific, Singapore, 2001.

M. A. Gallis and J. K. Harvey, "Modeling of Chemical Reactions in Hypersonic Rarefied Flow with DSMC", *Journal of Fluid Mechanics*, **312**, pp. 149-172, 1996.

M. A. Gallis and J. K. Harvey, "On the Modeling of Thermochemical Non-Equilibrium in Particle Simulations", *Physics of Fluids*, **10**, (6), pp. 1344-1358, 1998.

M. A. Gallis, J. R. Torczynski, and D. J. Rader, "Molecular Gas Dynamics Observations of Chapman-Enskog Behavior and Departures Therefrom in Nonequilibrium Gases", *Physical Review E*, **69**, 042201, 2004.

M. A. Gallis, J. R. Torczynski, D. J. Rader, M. Tij, and A. Santos, "Normal Solutions of the Boltzmann Equation for Highly Nonequilibrium Fourier and Couette Flow", *Physics of Fluids*, **18**, 017104, 2006.

R. N. Gupta, J. M. Yos, R. A. Thompson, and K.-P., Lee, "A Review of Reaction Rates and Thermodynamics and Transport Properties from an 11-Species Air Model for Chemical and Thermal Nonequilibrium Calculation to 30,000 K", NASA Reference Publication 1232, August 1990.

R. D. Levine and R. B. Bernstein, *Molecular Reaction Dynamics and Chemical Reactivity*, Oxford University Press, 1987.

G. Herzberg, *Molecular Spectra and Molecular Structure*, Vol. I, D. Van Nostrand Company, New York, NY, 1939.

J. O. Hirschfelder, C. F. Curtiss, and R. B. Bird, *Molecular Theory of Gases and Liquids*, John Wiley & Sons, New York, NY, 1954.

H. S. Johnston, "Gas Phase Reaction Kinetics of Neutral Oxygen Species", NSRDS-NBS 20, 1968.

R. G. Lord, "Modeling Vibrational Energy Exchange of Diatomic Molecules using the Morse Interatomic Potential", *Physics of Fluids,* **10, (**3), pp. 742-746, 1998.

P. M. Marriott and J. K. Harvey, "A New Approach for Modeling Energy Exchange and Chemical Reactions in the Direct Simulation Monte Carlo Method", *Rarefied Gas Dynamics*, Ed. A. Beylich, Aachen, pp. 784-791, 1990.

D. A. McQuarrie and J. D. Simon, *Physical Chemistry, A Molecular Approach*, University Science Books, Sausalito, CA, 1997.

J. P. Monat, R. K. Hanson, and C. H. Kruger, "Shock Tube Determination of the Rate Coefficient for the Reaction $N_2 + O \rightarrow NO + N$", *Proceedings of the 17th Symposium (International) on Combustion*, pp. 543-552, 1978.

C. Park, *Nonequilibrium Hypersonic Aerothermodynamics*, John Wiley & Sons, New York, NY, 1990.

C. Park, "Review of Chemical-Kinetic Problems of Future NASA Missions, I: Earth Entries", *Journal of Thermophysics and Heat Transfer*, **7**, (3), pp. 385-398, 1993.

M. Ju. Pogosbekian, A. L. Sergievskaya, and S. A. Losev, "Verification of Theoretical models of Chemical Exchange Reactions on the Basis of Quasi-Classical Trajectory Calculations", *Chemical Physics,* **328**, pp. 371-378, 2006.

F. Reif, *Fundamentals of Statistical and Thermal Physics*, McGraw-Hill Book Company, New York, NY, 1965.

A. L. Sergievskaya, E. A. Kovach, S. A. Losev, and N. M. Kuznetsov, "Thermal Nonequilibrium Models for Dissociation and Chemical Exchange Reactions at High Temperatures", AIAA Paper 96-1895, American Institute of Aeronautics and Astronautics, Reston, VA, 1996.

S. P. Sharma, W. M. Huo, and C. Park, "The Rate Parameters for Coupled Vibrational-Dissociation in a Generalized SSH Approximation", AIAA Paper 88-2714, American Institute of Aeronautics and Astronautics, Reston, VA, 1988.

D. C. Wadsworth and I. J. Wysong, Vibrational favoring effect in DSMC dissociation models, *Physics of Fluids*, **9** (12), pp. 3873-3884, 1997.

W. A. Wagner, "Convergence Proof for Bird's Direct Simulation Monte Carlo Method for the Boltzmann Equation", *Journal of Statistical Physics*, **66**, pp. 1011-1044, 1992.

C. K. Westbrook and F. L. Dryer, "Chemical Kinetic Modeling of Hydrocarbon Combustion", *Progress in Energy and Combustion Science*, **10**, pp. 1-57, 1984.

I. J. Wysong, R. A. Dressler, Y. H. Chiu, and I. D. Boyd, "Direct Simulation Monte Carlo Dissociation Model Evaluation: Comparison to Measured Cross Sections", *Journal of Thermophysics and Heat Transfer*, **16**, p. 1, 2002.

8. DISTRIBUTION

1	MS0384	A. C. Ratzel	01500	
1	MS0836	J. S. Lash	01510	
1	MS0836	S. P. Kearney	01512	
1	MS0346	D. J. Rader	01513	
10	MS0346	M. A. Gallis	01513	
1	MS0346	E. S. Piekos	01513	
1	MS0346	J. R. Torczynski	01513	
1	MS0825	J. L. Payne	01515	
1	MS0825	F. G. Blottner	01515	
1	MS0825	R. B. Bond	01515	
1	MS0825	D. W. Kuntz	01515	
1	MS0825	D. L. Potter	01515	
1	MS0836	M. M. Hopkins	01516	
1	MS0836	B. Hassan	01541	
1	MS1322	P. S. Crozier	01435	
1	MS0754	P. V. Brady	06310	
1	MS0899	Technical Library	09536	(electronic copy)
1	MS0123	D. L. Chavez, LDRD Office	01011	


Sandia National Laboratories